Accepted Manuscript

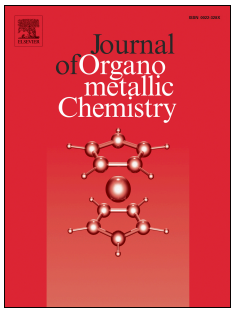

New diorganotin(IV) complexes of salicylaldehyde based hydrazones bearing furan heterocycle moiety: X-ray structural investigation of dimethyltin(IV) and diphenyltin(IV) complexes

Sundeep Kumar, Mala Nath

PII: S0022-328X(17)30735-0

DOI: 10.1016/j.jorganchem.2017.12.037

Reference: JOM 20232

To appear in: *Journal of Organometallic Chemistry*

Received Date: 17 October 2017

Revised Date: 19 December 2017

Accepted Date: 30 December 2017

Please cite this article as: S. Kumar, M. Nath, New diorganotin(IV) complexes of salicylaldehyde based hydrazones bearing furan heterocycle moiety: X-ray structural investigation of dimethyltin(IV) and diphenyltin(IV) complexes, *Journal of Organometallic Chemistry* (2018), doi: 10.1016/j.jorganchem.2017.12.037.

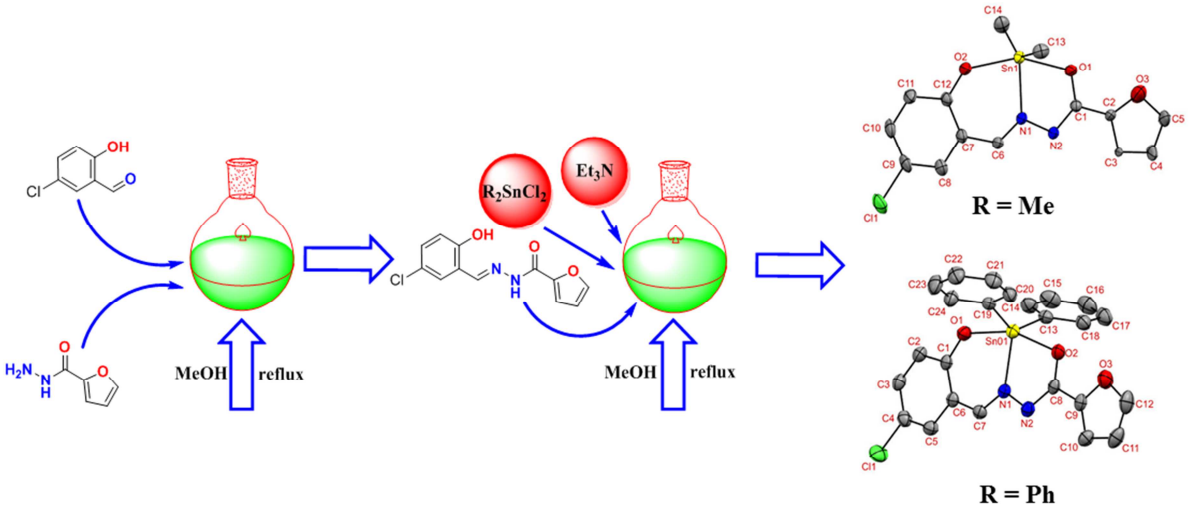

New diorganotin(IV) complexes of salicylaldehyde based hydrazones bearing furan heterocycle moiety: X-ray structural investigation of dimethyltin(IV) and diphenyltin(IV) complexes

Sundeep Kumar[a] and Mala Nath[a*]

[a] *Department of Chemistry, Indian Institute of Technology Roorkee, Roorkee-247667, Uttarakhand, India.*

* *Corresponding author.* Tel. *:* +91 1332 285797; Fax: +91 1332 73560.

E-mail address: malanfcy@iitr.ernet.in (M. Nath)

Abstract

Some new diorganotin(IV) derivatives formulated as R_2SnL (where R = Me, Bu, Ph and Oct) were obtained upon treatment of diorganotin(IV) precursors with acylhydrazones [H_2L^a = N'-(2-hydroxy-3-methoxybenzylidene)furan-2-carbohydrazide, H_2L^b = N'-(5-chloro-2-hydroxy-benzylidene)furan-2-carbohydrazide and H_2L^c = N'-(2-hydroxy-5-nitrobenzylidene)furan-2-carbohydrazide] derived from Schiff base condensation of furan-2-carbohydrazide and substituted salicylaldehydes in methanol in appropriate molar ratio. The enolic tridentate chelating mode of the acylhydrazones towards the diorganotin moieties $[R_2Sn(IV)]^{2+}$ was ascertained by micro-analysis and various spectroscopic techniques viz., Fourier-transform infrared (FT-IR), multinuclear (^1H, ^{13}C and ^{119}Sn) magnetic resonance (NMR) and electrospray ionization mass (ESMS) spectrometry. The single crystal X-ray diffraction investigation of Me_2SnL^b and Ph_2SnL^b demonstrates that they crystallize in monoclinic space groups 'P 2_1' and 'P 2_1/c' respectively, and comprised of crystallographically discrete 2 and 4 molecules in their respective unit cells. Both mononuclear complexes adopt a highly distorted square-pyramidal geometry (SP) wherein the imine nitrogen preferably occupies the apical site whereas the more electronegative enolic and phenolic oxygen atoms of the ligand and two carbon atoms of the methyl/phenyl groups of the organotin(IV) moiety align themselves equatorially around the five-coordinated tin center in a square plane. Diorganotin(IV) derivatives were also analyzed in air by thermo-gravimetric (TG, DTG and DTA) techniques to elucidate their thermal stability and decomposition trends.

1. Introduction

In metal coordination chemistry, hydrazones have been widely recognized as versatile

ligands because they are endowed with remarkable chelating behaviour and structural flexibility in many metal complexes. In the last few years, numerous acylhydrazones were documented and evaluated as potential drug candidates to prevent the menace of the life threatening diseases such as malaria, cancer and β-thalas semia major (Fe-overload disease) etc. [1-3]. Recently, many organotin(IV) complexes of acylhydrazones were evaluated to exhibit promising antibacterial and antitumor activities against the standard drugs [4,5]. Further, the interactions of organotin(IV) derivatives of the acylhydrazones with DNA/BSA were investigated by various spectroscopic techniques to explore their mode of actions as metal-based anticancer drugs [6]. The mode of biochemical action of the organotin(IV) complexes were reported to be governed by a variation in their structures, coordination state, nature of the ligating donor atoms and number/nature of the alkyl/aryl groups bound to the tin atom [7,8]. Meanwhile, several organotin(IV) derivatives of acylhydrazones were also investigated to exhibit structural diversity viz., distorted trigonal-bipyramidal (TBP) or square-pyramidal (SP) geometry around a penta-coordinated tin atom consisting of the imine N atom invariably at the equatorial and axial sites respectively, and a pentagonal-bipyramidal geometry for a seven-coordinated tin atom located in a C_2O_4N core along with two alkyl/aryl groups aligned trans to each other wherein organotin(IV) complexes acted as a Lewis acid to accommodate the electron density either from molecules of employed solvents or donor atoms of other molecules resulting in a weakly-bridged dimers with weak Sn$^{\cdots}$O bonding interactions [9-11]. Furthermore, fascinating 1D chains, 2D sheets and 2D/3D networks supramolecular structures were occasionally observed as a consequence of self-assembly of the organometallic subunits through intramolecular O-H$^{\cdots}$X or C-H$^{\cdots}$X (X = O, N or F) hydrogen bonding interactions, which were reported to be unaffected by the variation of the aryl groups of the Schiff base ligands [12,13]. Moreover, many ligating possibilities of acylhyrazones of ortho-hydroxyaldehydes containing a third potential coordination site were reported on the basis of availability of the varying sets of donor sites viz., monobasic ON bidentate, monobasic ONO tridentate or a dibasic ONO tridentate chelation [14,15]. The inadequate work reported on the structural chemistry of the diorganotin(IV) complexes of the furancarboxylic acid hydrazones [10,16], and interesting keto-enol tautomerization imparting structural flexibility to them in literature profoundly prompted us to design new diorganotin(IV) derivatives of salicylaldehyde based hydrazones bearing furan heterocycle moiety. Herein, we have highlighted the synthesis and characterization of eleven new diorganotin(IV) derivatives formulated as $R_2SnL^{a\text{-}c}$ (where R = Me,

Bu, Ph and Oct) of documented acylhydrazones derived from furan-2-carbohydrazide and substituted salicylaldehyde in the presence of trimethylamine base (a mild proton abstractor). The coordination mode of the ligands towards the various organotin(IV) moieties was ascertained by investigating the dimethyl- and diphenyl organotin(IV) complexes, Me_2SnL^b and Ph_2SnL^b with single crystal X-ray diffraction crystallographic analysis.

Insert Fig. 1

2. Experimental

2.1. Materials

Organotin precursors viz., dimethyltin(IV) dichloride, diphenyltin(IV) dichloride, di-*n*-butyltin(IV) dichloride and di-*n*-octyltin(IV) oxide were procured from Sigma Aldrich and Merck-Schuchardt respectively. Furoic acid hydrazide (Sigma Aldrich), *o*-vanillin (Sigma Aldrich), 5-chlorosalicylaldehyde (Sigma Aldrich), 5-nitrosalicylaldehyde (Hi-Media), and triethylamine (AR grade, Rankem) etc. were utilized as received commercially. Methanol (LR grade, Rankem) was employed as a solvent without its further purification throughout the synthesis.

2.2. Physical measurements

All solid compounds, compactly packed in one-end sealed glass capillaries were used to observe their melting points on an OptiMelt Automated Melting Point System, Stanford Research Systems instrument equipped with a Digital Image Processing Technology, and melting points so obtained were invariably uncorrected. Solid samples of all synthesized compounds were carefully loaded on a VarioMicro CHNS Elemental analyzer instrument (Ser. No.: 15136064) in order to perform the micro-analysis for the percentage of C, H and N contents. Dried and uniformly pressed potassium bromide pellets, provided by dispersing fine powder of solid compounds in a spectroquality KBr (matrix) were employed to obtain their IR spectra in the frequency range of 4000 to 400 cm^{-1} on a Nicolet 6700 Nexus FT-IR Spectrophotometer. Acquisition of all multi-nuclear (^1H, ^{13}C, and ^{119}Sn) magnetic resonance spectral data of studied compounds were acquired in deuterated NMR solvents viz. deutero chloroform ($CDCl_3$) and deutero dimethyl sulfoxide ($(CD_3)_2SO$) on a Bruker Avance (Bruker Bio Spin GmbH, 500.133 MHz) FT NMR spectrometer and a JEOL Delta (JNM-ECX400II, 400 MHz) FT-NMR spectrophotometer at ambient temperature. All ^1H and ^{13}C NMR spectra were referred to the residual solvent signals, assigned

invariably at δ = 7.26 and 2.5 for proton, and 77.16 and 39.52 ppm for carbon resonances when acquired in $CDCl_3$ and $(CD_3)_2SO$ [17], respectively. Electro-spray ionization (ES-MS) mass spectral analysis was preferably executed in a positive ion detection mode, and ES-MS mass spectra were collected from the SAIF, Central Drug Research Institute, Lucknow, India. Single crystal X-ray diffraction data for the compounds Me_2SnL^b and Ph_2SnL^b were collected on a Bruker Kappa Apex-II charge-coupled device (CCD) detector diffractometer equipped with a graphite monochromated Mo Kα radiation (λ = 0.71073 Å) source at ambient temperature at the Institute Instrumentation Centre (IIC), Indian Institute of Technology Roorkee (IITR), Roorkee, India. Acquisition of diffraction data was acquired by mounting suitable yellow crystals of dimensions 0.40 × 0.37 × 0.35 mm and 0.35 × 0.33 × 0.37 mm for Me_2SnL^b and Ph_2SnL^b, respectively. The diffraction data was processed using Direct method with SIR-92 programme in order to obtain the solutions for the crystal structures [18]. Anisotropic refinement of all non-hydrogen atoms was achieved by "full matrix least-squares calculations based on F^2" using SHELXL97 programme [19]. The hydrogen atoms were located and positioned geometrically, and were constrained to ride on their respective parent atoms. Illustrative ORTEP and molecular packing diagrams were generated using Mercury, version 3.9 software. Thermograms of diorganotin(IV) derivatives were attained on a Perkin-Elmer (Pyris Diamond) thermal analyzer by their controlled pyrolysis (heating rate, 20 ºC/min) in a platinum crucible using alumina powder as a reference material in the temperature range 20 to 1000 ºC with inflow air rate of 200 ml/min, at I. I. C., IITR.

2.3. Synthesis

Acylhydrazones, N'-(2-hydroxy-3-methoxybenzylidene)furan-2-carbohydrazide (H_2L^a), N'-(5-chloro-2-hydroxybenzylidene)furan-2-carbohydrazide (H_2L^b) and N'-(2-hydroxry-5-nitro-benzylidene)furan-2-carbohydrazide (H_2L^c), derived from the facile Schiff base condensation of furan-2-carbohydrazide and substituted salicylaldehydes, and their respective diorganotin(IV) derivatives were obtained as described in the following sections:

2.3.1. Synthesis of N'-(2-hydroxy-3-methoxybenzylidene)furan-2-carbohydrazide (H_2L^a)

To a stirred solution of furoic acid hydrazide (0.63 g, 5 mmol) in 15 mL of methanol was dropwise added *o*-vanillin (0.7608 g, 5 mmol) dissolved in 15 mL methanol. After stirring for 30 min on a magnetic stirrer, the bright yellow solution was refluxed for ca. 5 h on a water bath

under dry nitrogen atmosphere. The refluxed yellow solution was then allowed to attain ambient temperature, and subsequently refrigerated overnight, which gradually yielded a white crystalline solid by rigorous manual stirring for a while. The white crystalline ligand so precipitated was then carefully filtered under reduced pressure, washed with 20 mL of cold methanol, and dried in *vacuo* for further use.

White solid; Yield: 81%; m.p. 152-153 ºC; Anal. Calcd. for $C_{13}H_{12}N_2O_4$ (M. Wt. 260.25): C, 60.00; H, 4.65; N, 10.76. Found: C, 59.79; H, 5.01; N, 10.31; ES-MS (m/z): 301.0 $[(C_{13}H_{12}N_2O_4)+K]^+$; 283.0 $[(C_{13}H_{12}N_2O_4)+Na]^+$; 261.61/261.0862 $[(C_{13}H_{12}N_2O_4)+H]^+$; Selected FT-IR Data (KBr, ν_{max}/cm^{-1}): 3344, ν(O-H); 3202, ν(N-H); 1660, ν(C=O); 1610, $\nu(C=N)_{azomethine}$; ^{1}H NMR (500.13 MHz, $(CD_3)_2SO$, δ(ppm)): 3.82 (s, 3H, OCH_3); 6.71 (dd, 1H, H-2, $J_{H\text{-}H}$ = 3.5, 1.7 Hz); 6.86 (t, 1H, H-9, $J_{H\text{-}H}$ = 7.9 Hz); 7.03 (d, 1H, H-10, $J_{H\text{-}H}$ = 7.4 Hz); 7.14 (d, 1H, H-8, $J_{H\text{-}H}$ = 7.6 Hz); 7.32 (d, 1H, H-3, $J_{H\text{-}H}$ = 2.5 Hz); 7.96 (s, 1H, H-1); 8.66 (s, 1H, HC=N); 10.81 (s, 1H, HN-N); 12.08 (s, 1H, HOC); ^{13}C NMR (100.53 MHz, $(CD_3)_2SO$, δ(ppm)): 55.87, C-13; 112.25, C-2; 113.82, C-10; 115.30, C-3; 119.07, C-9; 119.13, C-7; 120.62, C-8; 146.13, C-1; 146.33, C-6; 147.09, C-4; 148.00, C-11; 148.05, C-12; 154.02, C-5.

2.3.2. Synthesis of N'-(5-chloro-2-hydroxybenzylidene) furan-2-carbohydrazide (H_2L^b)

It was synthesized by following the similar synthetic route as described in section 2.3.1 using furoic acid hydrazide (0.63 g, 5 mmol) and 5-chloro-2-hydroxybenzaldehyde (0.7828 g, 5 mmol).

White solid; Yield: 78%; m.p. 200-201 ºC; Anal. Calcd. for $C_{12}H_9ClN_2O_3$ (M. Wt. 264.67): C, 54.46; H, 3.43; N, 10.58. Found: C, 54.20; H, 3.91; N, 10.21; ES-MS (m/z): 286.9 $[(C_{12}H_9ClN_2O_3)+Na]^+$; 264.9/265.0368 $[(C_{12}H_9ClN_2O_3)+H]^+$; 123.8 $[(C_5H_4N_2O_2)]$; Selected FT-IR Data (KBr, ν_{max}/cm^{-1}): 3220, ν(O-H); 3135, ν(N-H); 1654, ν(C=O); 1625, $\nu(C=N)_{azomethine}$; ^{1}H NMR (500.13 MHz, $(CD_3)_2SO$, δ(ppm)): 6.71 (s, 1H, H-2); 6.94 (d, 1H, H-11, $J_{H\text{-}H}$ = 8.8 Hz); 7.31 (dd, 1H, H-3, $J_{H\text{-}H}$ = 8.8, 2.5 Hz); 7.32 (brs, 1H, H-10); 7.64 (d, 1H, H-8, $J_{H\text{-}H}$ = 2.6 Hz); 7.96 (d, 1H, H-1, $J_{H\text{-}H}$ = 1.0 Hz); 8.62 (s, 1H, HC=N); 11.14 (s, 1H, HN-N); 12.18 (s, 1H, HOC); ^{13}C NMR (100.53 MHz, $(CD_3)_2SO$, δ(ppm)): 112.72, C-2; 115.91, C-3; 118.73, C-7; C-11; 121.34, C-9; 123.54, C-8; 127.84, C-10; 131.34, C-1; 146.15, C-6; 146.70, C-4; 154.65, C-12; 156.44, C-5.

2.3.3. Synthesis of N'-(2-hydroxy-5-nitrobenzylidene) furan-2-carbohydrazide (H_2L^c)

To a stirred solution of furoic acid hydrazide (0.63 g, 5 mmol) in 15 mL of methanol was

dropwise added 2-hydroxy-5-nitrobenzaldehyde (0.7608 g, 5 mmol) dissolved in 15 mL methanol. After subsequent stirring for 20 min, the yellow solid immediately precipitated out. The reaction contents were stirred for 1 h additionally to ensure the completion of reaction. The yellow ligand so precipitated was then carefully filtered under reduced pressure, washed with 20 mL of methanol, and dried in *vacuo* for further use.

Yellow solid; Yield: 83%; m.p. 272-274 ºC; Anal. Calcd. for $C_{12}H_9N_3O_5$ (M. Wt. 275.22): C, 52.37; H, 3.30; N, 15.27. Found: C, 52.70; H, 3.34; N, 15.50; ES-MS (m/z): 298.0 $[(C_{12}H_9N_3O_5)+Na]^+$; 276.0/276.0618 $[(C_{12}H_9N_3O_5)+H]^+$; Selected FT-IR Data (KBr, ν_{max}/cm^{-1}): 3455, ν(O-H); 3276, ν(N-H); 1672, ν(C=O); 1636, $\nu(C=N)_{azomethine}$; ^{1}H NMR (500.13 MHz, $(CD_3)_2SO$, δ(ppm)): 6.71 (s, 1H, H-2); 6.94 (d, 1H, H-11, J_{H-H} = 8.8 Hz); 7.31 (dd, 1H, H-3, J_{H-H} = 8.8, 2.5 Hz); 7.32 (brs, 1H, H-10); 7.64 (d, 1H, H-8, J_{H-H} = 2.6 Hz); 7.96 (d, 1H, H-1, J_{H-H} = 1.0 Hz); 8.62 (s, 1H, HC=N); 11.14 (s, 1H, HN-N); 12.18 (s, 1H, HOC); ^{13}C NMR (100.53 MHz, $(CD_3)_2SO$, δ(ppm)): 112.72, C-2; 115.91, C-3; 118.73, C-7, C-11; 121.34, C-9; 123.54, C-8; 127.84, C-10; 131.34, C-1; 146.15, C-6; 146.70, C-4; 154.65, C-12; 156.44, C-5.

2.3.4. Synthesis of (N-(2-hydroxy-3-methoxybenzylidene)furan-2-carbohydrazonato)dimethyl-tin(IV)(Me_2SnL^a)

To a methanol (10 mL) solution of H_2L^a (0.1301 g, 0.5 mmol) was dropwise added Et_3N (0.1113 g, 1 mmol) in methanol (10 mL) with continuous stirring on a magnetic stirrer. A methanol (10 mL) solution of Me_2SnCl_2 (0.11 g, 0.5 mmol) was then gradually added to the stirred solution with the help of a dropping funnel. The resulting mixture was refluxed for 4 h under N_2 atmosphere on a water bath. The intense yellow colored solution so obtained was concentrated under reduced pressure till a yellow solid yielded which was subsequently filtered under vacuum. The yellow solid so obtained was recrystallized from methanol/petroleum ether (b.p. 40-60 ^{0}C) mixture (1:2 v/v), and dried in *vacuo*.

Me_2SnL^a: Yellow solid; Yield, 78%; m.p. 185-187 ºC; Anal. Calcd. for $C_{15}H_{16}N_2O_4Sn$ (M. Wt. 407.01): C, 44.27; H, 3.96; N, 6.88. Found: C, 44.68; H, 3.93; N, 7.08; ES-MS (m/z): 408.9 $[(C_{13}H_{10}N_2O_4)(Me_2Sn)+H]^+$; 282.9 $[(C_{13}H_{12}N_2O_4)+Na]^+$; 260.9 $[(C_{13}H_{12}N_2O_4)+H]^+$; Selected FT-IR Data (KBr, ν_{max}/cm^{-1}): 1619, $\nu(C=N)_{azomethine}$; 647, ν_{as}(Sn-C); 583, ν_s(Sn-C); 532, ν(Sn-O); 453, ν(Sn-N); ^{1}H NMR (500.13 MHz, $(CD_3)_2SO$, δ(ppm)): 0.69 (s, 6H, H-*α*, $^2J(^{119}Sn-^1H)$ = 90.5

Hz, ∟C-Sn-C =145.8°); 3.72 (s, 3H, OCH_3); 5.58-6.63 (m, 2H, H-2, H-9); 6.95 (d, 2H, H-3, H-10, $J_{H\text{-}H}$ = 7.9 Hz); 6.98 (d, 1H, H-8, $J_{H\text{-}H}$ = 3.3 Hz); 7.79 (brs, 1H, H-1); 8.74 (s, 1H, HC=N, $^3J(^{119}Sn\text{-}^1H)$ = 35 Hz); ^{13}C NMR (100.53 MHz, $(CD_3)_2SO$, δ(ppm)): 6.57, C-*α*; 55.41, C-13; 111.84, C-3; 113.26, C-2; 115.46, C-9; 115.60, C-10; 116.95, C-7; 125.83, C-8; 145.09, C-1; 148.04, C-4; 150.94, C-12; 154.11, C-11; 160.06, C-6; 161.48, C-5; ^{119}Sn NMR (149.08 MHz, $CDCl_3$, δ(ppm)): -150.44.

2.3.5. Synthesis of (N-(2-hydroxy-3-methoxybenzylidene)furan-2-carbohydrazonato)dibutyltin(IV) (Bu_2SnL^a)

It was synthesized by employing the similar synthetic route as described in section 2.3.4 using H_2L^a (0.1301 g, 0.5 mmol), Et_3N (0.1113 g, 1 mmol) and Bu_2SnCl_2 (0.1519 g, 0.5 mmol).

Bu_2SnL^a: Yellow solid; Yield, 71%; m.p. 101-102 ºC; Anal. Calcd. for $C_{21}H_{28}N_2O_4Sn$ (M. Wt. 491.17): C, 51.35; H, 5.75; N, 5.70. Found: C, 51.67; H, 5.94; N, 6.00; ES-MS (m/z): 515.0 $[(C_{13}H_{10}N_2O_4)(Bu_2Sn)+Na]^+$; 492.9 $[(C_{13}H_{10}N_2O_4)(Bu_2Sn)+H]^+$; 282.9 $[(C_{13}H_{12}N_2O_4)+Na]^+$; 261.0 $[(C_{13}H_{12}N_2O_4)+H]^+$; Selected FT-IR Data (KBr, ν_{max}/cm^{-1}): 1616, $\nu(C=N)_{azomethine}$; 553, ν(Sn-O); 518, ν(Sn-C); 441, ν(Sn-N); ^1H NMR (500.13 MHz, $CDCl_3$, δ(ppm)): 0.83 (t, 6H, H-*δ*, $^3J_{H\text{-}H}$ = 7.3 Hz); 1.28-1.37 (m, 4H, H-*β*); 1.50-1.66 (m, 8H, H-*α*, H-*γ*); 3.85 (s, 3H, OCH_3); 6.51 (s, 1H, H-2); 6.66 (t, 1H, H-9, $J_{H\text{-}H}$ = 7.8 Hz); 6.78 (d, 1H, H-10, $J_{H\text{-}H}$ = 8.0 Hz); 6.92 (d, 1H, H-3, $J_{H\text{-}H}$ = 7.5 Hz); 7.04 (d, 1H, H-8); 7.55 (s, 1H, H-1); 8.75 (s, 1H, HC=N, $^3J(^{119}Sn\text{-}^1H)$ = 41 Hz); ^{13}C NMR (100.53 MHz, $CDCl_3$, δ(ppm)): 13.68, C-*δ*; 23.19, C-*α*; 26.55, C-*γ*; 26.89, C-*β*; 55.38, C-13; 111.77, C-3; 113.95, C-2; 115.89, C-9; 116.34, C-10; 116.61, C-7; 126.00, C-8; 144.83, C-1; 147.85, C-4; 151.34, C-12; 157.54, C-11; 161.83, C-6; 162.72, C-5; ^{119}Sn NMR (149.08 MHz, $CDCl_3$, δ(ppm)): -187.53.

2.3.6. Synthesis of (N-(2-hydroxy-3-methoxybenzylidene)furan-2-carbohydrazonato)diphenyltin(IV) (Ph_2SnL^a)

To a methanol (10 mL) solution of H_2L^a (0.1301 g, 0.5 mmol) was dropwise added Et_3N (0.1113 g, 1 mmol) in methanol (10 mL) with continuous stirring under N_2 atmosphere. A methanol (10 mL) solution of Ph_2SnCl_2 (0.1719 g, 0.5 mmol) was then gradually added to the stirred solution with the help of a dropping funnel at ambient temperature. After subsequent stirring for 20 min, the yellow solid immediately precipitated out. The reaction contents were stirred for 3 h additionally to ensure the completion of reaction. The yellow compound was

carefully filtered under reduced pressure. The yellow solid so obtained was recrystallized from methanol/petroleum ether (b.p. 40-60 ^{0}C) mixture (1:2 v/v), and dried in *vacuo*.

Ph_2SnL^a: Yellow solid; Yield, 79%; m.p. 194-195 ºC; Anal. Calcd. for $C_{25}H_{20}N_2O_4Sn$ (M. Wt. 531.15): C, 56.53; H, 3.80; N, 5.27. Found: C, 56.51; H, 3.70; N, 5.31; ES-MS (m/z): 554.8 $[(C_{13}H_{10}N_2O_4)(Ph_2Sn)+Na]^+$; 532.7 $[(C_{13}H_{10}N_2O_4)(Ph_2Sn)+H]^+$; 282.9 $[(C_{13}H_{12}N_2O_4)+Na]^+$; 260.9 $[(C_{13}H_{12}N_2O_4)+H]^+$; Selected FT-IR Data (KBr, $\nu max/cm^{-1}$): 1612, $\nu(C=N)_{azomethine}$; 595, ν(Sn-O); 499, ν(Sn-C); 449, ν(Sn-N); ^{1}H NMR (500.13 MHz, $CDCl_3$, δ(ppm)): 3.98 (s, 3H, OCH_3); 6.57 (dd, 1H, H-2, $J_{H\text{-}H}$ = 8.0, 1.5 Hz); 6.72 (t, 1H, H-8, $J_{H\text{-}H}$ = 7.9 Hz); 6.81 (dd, 1H, H-9, $J_{H\text{-}H}$ = 8.0, 1.5 Hz); 7.03 (dd, 1H, H-3, $J_{H\text{-}H}$ = 7.8, 1.5 Hz); 7.25 (dd, 1H, H-10, $J_{H\text{-}H}$ = 3.4, 0.8 Hz); 7.59 (s, 1H, H-1); 7.40-7.43 (m, 6H, H-*β*, H-*γ*); 7.89 (dd, 4H, H-*α* $^3J_{H\text{-}H}$ = 8.2, 3.9 Hz, $^3J(^{119}Sn\text{-}^1H)$ = 86.0 Hz); 8.77 (s, 1H, HC=N, $^3J(^{119}Sn\text{-}^1H)$ = 50.1 Hz); ^{13}C NMR (100.53 MHz, $CDCl_3$, δ(ppm)): 56.87, C-13; 111.99, C-3; 114.91, C-2; 116.74, C-9; 116.96, C-10; 117.23, C-7; 126.23, C-8; 129.16, C-*β*; 130.84, C-*γ*; 136.49, C-*α*, $^2J(^{119}Sn\text{-}^{13}C)$ = 55.3 Hz; 140.01, C-*ipso*; 145.26, C-1, C-4, C-12; 152.04 C-11; 162.16, C-6; 162.51, C-5; ^{119}Sn NMR (149.08 MHz, $CDCl_3$, δ(ppm)): -329.52.

2.3.7. *Synthesis of (N-(2-hydroxy-3-methoxybenzylidene)furan-2-carbohydrazonato)dioctyltin(IV) (Oct_2SnL^a)*

A mixture of Oct_2SnO (0.1806 g, 0.5 mmol) and H_2L^a (0.1301 g, 0.5 mmol) in methanol (10 mL)/benzene (30 mL) mixture was refluxed for 8 h on a water bath under dry atmosphere, and water generated during the course of the reaction was azeotropically trapped with the help of Dean-Stark water separator. The refluxed intense yellow colored solution was filtered to remove the unreacted reactants, and concentrated under reduced pressure till a yellow solid yielded which was subsequently filtered under vacuum. The yellow solid so obtained was recrystallized from methanol/petroleum ether (b.p. 40-60 ^{0}C) mixture (1:2 v/v), and dried in *vacuo*.

Oct_2SnL^a: Yellow solid; Yield, 81%; m.p. 64-65 ºC; Anal. Calcd. for $C_{29}H_{44}N_2O_4Sn$ (M. Wt. 603.39): C, 57.73; H, 7.35; N, 4.64. Found: C, 58.03; H, 7.55; N, 4.63; ES-MS (m/z): 605.0 $[(C_{13}H_{10}N_2O_4)(Oct_2Sn)+H]^+$; 282.9 $[(C_{13}H_{12}N_2O_4)+Na]^+$; 260.9 $[(C_{13}H_{12}N_2O_4)+H]^+$; Selected FT-IR Data (KBr, $\nu max/cm^{-1}$): 1580, $\nu(C=N)_{azomethine}$; 535, ν(Sn-O); 456, ν(Sn-N); ^{1}H NMR (399.78 MHz, $CDCl_3$, δ(ppm)): 0.82 (t, 6H, H-*δ'*, $^3J_{H\text{-}H}$ = 7.0 Hz), 1.16-1.28 (m, 20H, H-*γ*-*γ'*), 1.46-1.52 (m, 8H, H-*α*, H-*β*), 3.84 (s, 3H, OCH_3); 6.49-6.51 (m, 1H, H-2); 6.65 (t, 1H, H-9, $J_{H\text{-}H}$ = 7.8 Hz); 6.77 (d, 1H, H-10, $J_{H\text{-}H}$ = 8.1 Hz); 6.91 (d, 1H, H-3, $J_{H\text{-}H}$ = 7.8 Hz); 7.03 (d, 1H, H-8, $J_{H\text{-}H}$ = 3.4 Hz);

7.54 (s, 1H, H-1); 8.73 (s, 1H, HC=N, $^{3}J(^{119}Sn\text{-}^{1}H)$ = 51.5 Hz); ^{13}C NMR (100.53 MHz, $CDCl_3$, δ(ppm)): 14.21, C-*δ′*; 22.74, C-*γ′*; 23.52, C-*α*; 24.76, C-*β*; 29.14, C-*α′*; 29.23, C-*δ*; 31.92, C-*β′*; 33.44, C-*γ*; 56.34, C-13; 111.79, C-3; 113.94, C-2; 115.88, C-9; 116.35, C-10; 116.65, C-7; 125.99, C-8; 144.80, C-1; 147.92, C-4; 157.38, C-12; 157.57, C-11; 161.80, C-6; 162.73, C-5; ^{119}Sn NMR (149.08 MHz, $CDCl_3$, δ(ppm)): -187.74.

2.3.8. Synthesis of (N-(5-chloro-2-oxybenzylidene)furan-2-carbohydrazonato)dimethyltin(IV) (Me_2SnL^b)

To a methanol (10 mL) solution of H_2L^b (0.1323 g, 0.5 mmol) was dropwise added Et_3N (0.1113 g, 1 mmol) in methanol (10 mL) with continuous stirring under N_2 atmosphere. A methanol (10 mL) solution of Me_2SnCl_2 (0.11 g, 0.5 mmol) was then gradually added to the stirred solution with the help of a dropping funnel. After stirring for 20 min, the yellow solid immediately precipitated out. The reaction contents were stirred for 3 h additionally to ensure the completion of reaction. The yellow compound was carefully filtered under reduced pressure. The yellow solid so obtained was recrystallized from methanol/petroleum ether (b.p. 40-60 ^{0}C) mixture (1:2 v/v), and dried in *vacuo*.

Me_2SnL^b: Greenish yellow solid; Yield, 78%; m.p. 244-246 ºC; Anal. Calcd. for $C_{14}H_{13}ClN_2O_3Sn$ (M. Wt. 411.43): C, 40.87; H, 3.18; N, 6.81. Found: C, 41.49; H, 3.08; N, 6.95; ES-MS (m/z): 412.8/412.9700 $[(C_{12}H_9ClN_2O_3)(Me_2Sn)+H]^+$; 286.9 $[(C_{12}H_9ClN_2O_3)+Na]^+$; 264.9 $[(C_{12}H_9ClN_2O_3)+H]^+$; Selected FT-IR Data (KBr, ν_{max}/cm^{-1}):1583 $\nu(C=N)_{azomethine}$; 624, ν_{as}(Sn-C); 532, ν_s(Sn-C); 494, ν(Sn-O); 435, ν(Sn-N); ^{1}H NMR (500.13 MHz, $(CD_3)_2SO$, δ(ppm)): 0.69 (s, 6H, H-*α*, $^{2}J(^{119}Sn\text{-}^{1}H)$ = 90.0 Hz, ∟C-Sn-C =145.0°); 6.61 (dd, 1H, H-2, $J_{H\text{-}H}$ = 3.4, 1.7 Hz); 6.67 (d, 1H, H-11, $J_{H\text{-}H}$ = 8.9 Hz); 7.01 (d, 1H, H-3, $J_{H\text{-}H}$ = 3.4 Hz); 7.26 (dd, 1H, H-10, $J_{H\text{-}H}$ = 8.9, 2.8 Hz); 7.46 (d, 1H, H-8, $J_{H\text{-}H}$ = 2.8 Hz); 7.81 (brs, 1H, H-1); 8.74 (s, 1H, HC=N, $^{3}J(^{119}Sn\text{-}^{1}H)$ = 45 Hz); ^{13}C NMR (100.53 MHz, $(CD_3)_2SO$, δ(ppm)): 6.55, C-*α*; 111.91, C-3; 113.60, C-2; 118.52, C-11; 119.18, C-7; 122.98, C-9; 132.66, C-8; 133.72, C-10; 145.31, C-1; 147.85, C-4; 158.47, C-6; 161.82, C-5; 164.33, C-12; ^{119}Sn NMR (149.08 MHz, $CDCl_3$, δ(ppm)): -149.26.

2.3.9. Synthesis of (N-(5-chloro-2-oxybenzylidene)furan-2-carbohydrazonato)dibutyltin(IV) (Bu_2SnL^b)

It was synthesized by employing the similar synthetic route as described in section 2.3.4 using H_2L^b (0.1323 g, 0.5 mmol), Et_3N (0.1113 g, 1 mmol) and Bu_2SnCl_2 (0.1519 g, 0.5 mmol).

Bu_2SnL^b: Greenish yellow solid; Yield, 75%; m.p. 94-96 ºC; Anal. Calcd. for $C_{20}H_{25}ClN_3O_3Sn$ (M. Wt. 495.59): C, 48.47; H, 5.08; N, 5.65. Found: C, 48.53; H, 5.26; N, 5.83; ES-MS (m/z): 497.07 $[(C_{12}H_9ClN_2O_3)(Bu_2Sn)+H]^+$; Selected FT-IR Data (KBr, ν_{max}/cm^{-1}): 1580, $\nu(C=N)_{azomethine}$; 559, ν(Sn-O); 509, ν(Sn-C); 450, ν(Sn-N); ^{1}H NMR (500.13 MHz, $(CD_3)_2SO$, δ(ppm)): 0.75 (t, 6H, H-*δ*, $^3J_{H\text{-}H}$ = 7.3 Hz); 1.19-1.27 (m, 4H, H-*β*); 1.36-1.52 (m, 8H, H-*α*, H-*γ*); 6.61 (dd, 1H, H-2, $J_{H\text{-}H}$ = 3.4, 1.7 Hz); 6.66 (d, 1H, H-11, $J_{H\text{-}H}$ = 8.9 Hz); 7.00 (d, 1H, H-3, $J_{H\text{-}H}$ = 3.3 Hz); 7.25 (dd, 1H, H-10, $J_{H\text{-}H}$ = 8.9, 2.8 Hz); 7.45 (d, 1H, H-8, $J_{H\text{-}H}$ = 2.8 Hz); 7.81 (brs, 1H, H-1); 8.77 (s, 1H, HC=N, $^3J(^{119}Sn\text{-}^1H)$ = 47.0 Hz); ^{13}C NMR (100.53 MHz, $CDCl_3$, δ(ppm)): 13.70, C-*δ*; 22.72, C-*α*; 26.58, C-*γ*; 26.87, C-*β*; 111.88, C-3; 114.39, C-2; 117.46, C-11; 121.29, C-7; 122.31, C-9; 132.44, C-8; 135.11, C-10; 145.06, C-1; 147.66, C-4; 160.25, C-6; 163.02, C-5; 165.56, C-12; ^{119}Sn NMR (149.08 MHz, $CDCl_3$, δ(ppm)): -187.36.

2.3.10. Synthesis of (N-(5-chloro-2-oxybenzylidene)furan-2-carbohydrazonato)diphenyltin(IV) (Ph_2SnL^b)

It was synthesized by employing the similar synthetic route as described in section 2.3.6 using H_2L^b (0.1323 g, 0.5 mmol), Et_3N (0.1113 g, 1 mmol) and Ph_2SnCl_2 (0.1719 g, 0.5 mmol).

Ph_2SnL^b: Greenish yellow solid; Yield, 82%; m.p. 208-210 ºC; Anal. Calcd. for $C_{24}H_{17}ClN_2O_3Sn$ (M. Wt. 535.57): C, 53.82; H, 3.20; N, 5.23. Found: C, 54.06; H, 3.09; N, 5.32; ES-MS (m/z): 536.7/536.1647 $[(C_{12}H_9ClN_2O_3)(Ph_2Sn)+H]^+$; 288.9 $[(C_{12}H_9ClN_2O_3)+Na]^+$; 264.9 $[(C_{12}H_9ClN_2O_3)+H]^+$; Selected FT-IR Data (KBr, $\nu max/cm^{-1}$): 1593 $\nu(C=N)_{azomethine}$; 556, ν(Sn-O); 448, ν(Sn-N); ^{1}H NMR (500.13 MHz, $CDCl_3$, δ(ppm)): 6.58 (dd, 1H, H-2, $J_{H\text{-}H}$ = 3.4, 1.7 Hz); 7.04 (d, 1H, H-11, $J_{H\text{-}H}$ = 9.0 Hz); 7.13 (d, 1H, H-3, $J_{H\text{-}H}$ = 2.7 Hz); 7.27 (s, 1H, H-10); 7.34 (dd, 1H, H-10, $J_{H\text{-}H}$ = 8.9, 2.7 Hz); 7.42-7.44 (m, 6H, H-*β*, H-*γ*); 7.61 (brs, 1H, H-1); 7.83 (dd, 4H, H-*α*, $^3J_{H\text{-}H}$ = 6.3, 3.0 Hz, $^3J(^{119}Sn\text{-}^1H)$ = 86.0 Hz); 8.69 (s, 1H, HC=N, $^3J(^{119}Sn\text{-}^1H)$ = 49.5 Hz); ^{13}C NMR (100.53 MHz, $CDCl_3$, δ(ppm)): 111.94, C-3; 115.25, C-2; 117.57, C-11; 122.06, C-7; 123.75, C-9, 129.13, C-*β*; 130.93, C-*γ*; 132.69, C-8, 135.42, C-10, 136.26, C-*α*, $^2J(^{119}Sn\text{-}^{13}C)$ = 57.2 Hz; 138.48, C-*ipso*; 145.42, C-1; 147.46, C-4; 160.52, C-6; 162.75, C-5, 165.64, C-12; ^{119}Sn NMR (149.08 MHz, $CDCl_3$, δ(ppm)): -331.32.

2.3.11. Synthesis of (N-(5-nitro-2-oxybenzylidene)furan-2-carbohydrazonato)dimethyltin(IV) (Me_2SnL^c)

It was synthesized by employing the similar synthetic route as described in section 2.3.4

using H_2L^c (0.1376 g, 0.5 mmol), Et_3N (0.1113 g, 1 mmol) and Me_2SnCl_2 (0.11 g, 0.5 mmol).

Me_2SnL^c: Yellow solid; Yield, 81%; m.p. 318 ºC (dec.); Anal. Calcd. for $C_{14}H_{13}N_3O_5Sn$ (M. Wt. 421.98): C, 39.85; H, 3.11; N, 9.96. Found: C, 40.24; H, 3.00; N, 10.08; ES-MS (m/z): 423.0 $[(C_{12}H_9N_3O_5)\ (Me_2Sn)+H]^+$; 275.9 $[(C_{12}H_9N_3O_5)+H]^+$; Selected FT-IR Data (KBr, ν_{max}/cm^{-1}):1614 $\nu(C=N)_{azomethine}$; 618, ν_{as}(Sn-C); 518, ν_s(Sn-C); 494, ν(Sn-O); 450, ν(Sn-N); ^{1}H NMR (500.13 MHz, $(CD_3)_2SO$, δ(ppm)): 0.75 (s, 6H, H-*α*, $^2J(^{119}Sn\text{-}^1H)$ = 96.0 Hz, ∟C-Sn-C = 155.0°); 6.63 (dd, 1H, H-2, $J_{H\text{-}H}$ = 3.4, 1.7 Hz); 6.69 (d, 1H, H-3, $J_{H\text{-}H}$ = 9.3 Hz); 7.03 (d, 1H, H-11, $J_{H\text{-}H}$ = 3.4 Hz); 7.83 (s, 1H, H-1); 8.07 (dd, 1H, H-10, $J_{H\text{-}H}$ = 9.3, 3.0 Hz); 8.85 (d, 1H, H-8, $J_{H\text{-}H}$ = 3.0 Hz); 8.86 (s, 1H, HC=N, $^3J(^{119}Sn\text{-}^1H)$ = 35.5 Hz); ^{13}C NMR (100.53 MHz, $(CD_3)_2SO$, δ(ppm)): 8.90, C-*α*; 112.04, C-3; 113.93, C-2; 117.19, C-11; 121.97, C-7; 128.80, C-8; 131.65, C-10; 136.22, C-9; 145.54, C-1; 147.75, C-4; 158.19, C-6; 161.94, C-5; 171.61, C-12; ^{119}Sn NMR (149.08 MHz, $CDCl_3$, δ(ppm)): -147.78.

2.3.12. Synthesis of (N-(5-nitro-2-oxybenzylidene)furan-2-carbohydrazonato)dibutyltin(IV) (Bu_2SnL^c)

It was synthesized by employing the similar synthetic route as described in section 2.3.4 using H_2L^c (0.1376 g, 0.5 mmol), Et_3N (0.1113 g, 1 mmol) and Bu_2SnCl_2 (0.1519 g, 0.5 mmol).

Bu_2SnL^c: Yellow solid; Yield, 75%; m.p. 120-122 ºC; Anal. Calcd. for $C_{20}H_{25}N_3O_5Sn$ (M. Wt. 506.15): C, 47.46; H, 4.98; N, 8.30. Found: C, 47.22; H, 4.85; N, 8.51; ES-MS (m/z): 507.8/508.0884 $[(C_{12}H_9N_3O_5)\ (Bu_2Sn)+H]^+$; 297.8 $[(C_{12}H_9N_3O_5)+Na]^+$; Selected FT-IR Data (KBr, ν_{max}/cm^{-1}): 1613, $\nu(C=N)_{azomethine}$; 588, ν(Sn-O); 521, ν(Sn-C); 488, ν(Sn-N); ^{1}H NMR (500.13 MHz, $(CD_3)_2SO$, δ(ppm)): 0.73 (t, 6H, H-*δ*, $^3J_{H\text{-}H}$ = 7.3 Hz); 1.17-1.24 (m, 4H, H-*β*); 1.38-1.47 (m, 8H, H-*α*, H-*γ*); 6.63 (dd, 1H, H-2, $J_{H\text{-}H}$ = 3.4, 1.7 Hz); 6.69 (d, 1H, H-11, $J_{H\text{-}H}$ = 9.3 Hz); 7.03 (d, 1H, H-3, $J_{H\text{-}H}$ = 3.4 Hz); 7.84 (s, 1H, H-1); 8.07 (dd, 1H, H-10, $J_{H\text{-}H}$ = 9.3, 3.0 Hz); 8.45 (d, 1H, H-8, $J_{H\text{-}H}$ = 3.0 Hz); 8.95 (s, 1H, HC=N); ^{13}C NMR (100.53 MHz, $(CD_3)_2SO$, δ(ppm)): 13.54, C-*δ*; 25.55, C-*α*; 26.69, C-*γ*; 27.78, C-*β*; 111.98, C-3; 113.79, C-2; 116.96, C-11; 121.73, C-7; 128.91, C-8; 131.77, C-10; 136.09, C-9; 145.47, C-1; 147.67, C-4; 158.78, C-6; 162.35, C-5; 172.37, C-12; ^{119}Sn NMR (149.08 MHz, $CDCl_3$, δ(ppm)): -186.04.

2.3.13. Synthesis of (N-(5-nitro-2-oxybenzylidene)furan-2-carbohydrazonato)dipheyltin(IV) (Ph_2SnL^c)

It was synthesized by employing the similar synthetic route as described in section 2.3.6

using H_2L^c (0.1376 g, 0.5 mmol), Et_3N (0.1113 g, 1 mmol) and Ph_2SnCl_2 (0.1719 g, 0.5 mmol).

Ph_2SnL^c: Yellow solid; Yield, 82%; m.p. 296 ºC (dec.); Anal. Calcd. for $C_{24}H_{17}N_3O_5Sn$ (M. Wt. 546.13): C, 52.78; H, 3.14; N, 7.69. Found: C, 52.69; H, 3.16; N, 7.74; ES-MS (m/z): 548.00/548.0270 $[(C_{12}H_9N_3O_5)(Ph_2Sn)+H]^+$; Selected FT-IR Data (KBr, νmax/cm^{-1}): 1613 ν(C=N)azomethine; 574, ν(Sn-O); 479, ν(Sn-N); ^{1}H NMR (500.13 MHz, $CDCl_3$, δ(ppm)): 6.60 (dd, 1H, H-2, $J_{H\text{-}H}$ = 3.4, 1.8 Hz); 7.12 (d, 1H, H-3, $J_{H\text{-}H}$ = 9.3 Hz); 7.31 (dd, 1H, H-11, $J_{H\text{-}H}$ = 3.4, 0.6 Hz); 7.44-7.45 (m, 6H, H-*β*, H-*γ*); 7.64 (s, 1H, H-1); 7.81-7.83 (dd, 4H, H-*α*, $^3J_{H\text{-}H}$ = 6.0, 3.5 Hz, $^3J(^{119}Sn\text{-}^1H)$ = 90.0 Hz); 8.19 (d, 1H, H-10, $J_{H\text{-}H}$ = 2.8 Hz); 8.27 (dd, 1H, H-8, $J_{H\text{-}H}$ = 9.3, 2.9 Hz); 8.81 (s, 1H, HC=N, $^3J(^{119}Sn\text{-}^1H)$ = 48.5 Hz); ^{13}C NMR (100.53 MHz, $(CD_3)_2SO$ + $CDCl_3$, δ(ppm)): 111.94, C-3; 115.62, C-2; 115.92, C-11; 122.68, C-7; 129.06, C-*β*, C-8; 129.72, C-10; 130.92, C-*γ*; 135.79, C-*α*; 137.80; C-9; 138.33, C-*ipso*; 145.52, C-1; 146.77, C-4; 159.68, C-6; 162.89, C-5; 171.62, C-12; ^{119}Sn NMR (149.08 MHz, $CDCl_3$, δ(ppm)): -330.94.

2.3.14. Synthesis of (N-(5-nitro-2-oxybenzylidene)furan-2-carbohydrazonato)dioctyltin(IV) (Oct_2SnL^c)

It was synthesized by employing the similar synthetic route as described in section 2.3.7 using H_2L^c (0.1376 g, 0.5 mmol) and Oct_2SnO (0.1806 g, 0.5 mmol).

Oct_2SnL^c: Yellow solid; Yield, 77%; m.p. 93-95 ºC; Anal. Calcd. for $C_{28}H_{41}N_3O_5Sn$ (M. Wt. 618.4): C, 54.39; H, 6.68; N, 6.80. Found: C, 54.09; H, 6.61; N, 6.93; 620.0/620.2145 $[(C_{12}H_9N_3O_5)\ (Oct_2Sn)+H]^+$; 275.8 $[(C_{12}H_9N_3O_5)+H]^+$; Selected FT-IR Data (KBr, νmax/cm^{-1}): 1613 $\nu(C=N)_{azomethine}$; 491, ν(Sn-O); 424, ν(Sn-N); ^{1}H NMR (399.78 MHz, $CDCl_3$, δ(ppm)): 0.82 (t, 6H, H-*δ'*, $^3J_{H\text{-}H}$ = 7.0 Hz), 1.18-1.30 (m, 20H, H-*γ*-*γ'*), 1.57-1.66 (m, 8H, H-*α*, H-*β*), 6.53 (dd, 1H, H-2, $J_{H\text{-}H}$ = 3.7, 2.1 Hz); 6.75 (d, 1H, H-3, $J_{H\text{-}H}$ = 8.9 Hz); 7.08 (d, 1H, H-11, $J_{H\text{-}H}$ = 3.4 Hz); 7.57 (s, 1H, H-1); 8.14 (s, 1H, H-10); 8.16 (s, 1H, H-8); 8.77 (s, 1H, HC=N, $^3J(^{119}Sn\text{-}^1H)$ = 39.2 Hz); ^{13}C NMR (100.53 MHz, $CDCl_3$, δ(ppm)): 14.19, C-*δ'*; 22.72, C-*γ'*; 23.52, C-*α*; 24.65, C-*β*; 29.08, C-*α'*; 29.22, C-*δ*; 31.87, C-*β'*; 33.44, C-*γ*; 111.98, C-3; 114.98, C-2; 115.88, C-11; 122.45, C-7; 129.81, C-8; 131.01, C-10; 138.06, C-9; 145.31, C-1; 147.21, C-4; 159.85, C-6; 163.43, C-5; 171.99, C-12; ^{119}Sn NMR (149.08 MHz, $CDCl_3$, δ(ppm)): -186.48.

Insert Scheme 1

3. Results and discussion

3.1. Synthesis, reactivity and solid-state characteristics

Diorganotin(IV) derivatives of acylhydrazone Schiff base ligands viz., *N'-(2-hydroxy-3-methoxybenzylidene) furan-2-carbohydrazide (H_2L^a), N'-(5-chloro-2-hydroxybenzylidene) furan-2-carbohydrazide (H_2L^b) and N'-(2-hydroxry-5-nitrobenzylidene)furan-2-carbohydrazide (H_2L^c)*, were afforded after refluxing R_2SnCl_2 (R = Me, Bu and Ph) with ligands in methanol under N_2 atmosphere, and in the presence of an efficient proton abstractor, triethylamine which facilitates the deprotonation of ligand in 0.5 : 0.5 : 1 molar ratio. However, dioctyltin(IV) derivatives were obtained on refluxing Oct_2SnO with ligands in 0.5 : 0.5 molar ratio in methanol/benzene mixture (1:3 v/v), and by ensuring the simultaneous azeotropic removal of water from the reaction mixture as it is formed as described in the Experimental section (Scheme 2). All diorganotin(IV) derivatives are yellow solids, air-stable, and exhibit solubility in common organic solvents such as methanol, ethanol, chloroform and dimethylsulfoxide. The analytical data, incorporated in Experimental section clearly implies a 1:1 metal-to-ligand molar ratio in the synthesized diorganotin(IV) derivatives. In all of the organotin(IV) derivatives, coordination of the ligand to organotin(IV) moiety may be visualized through its imine nitrogen, enolic oxygen and phenolic oxygen atoms after feasible enolisation and deprotonation during the reaction, leading to a highly distorted square-pyramidal geometry (as illustrated in Fig. 2 and 4) at tin atom which is ascertained by X-ray structural investigation of Me_2SnL^b and Ph_2SnL^b as described below.

Insert Scheme 2

3.2. Single crystal X-ray structural characterization

Shinning yellow needle-like and block-like crystals of adequate size and quality were conveniently produced after slow evaporation of solvent from the respective concentrated solutions of Me_2SnL^b and Ph_2SnL^b in methanol in perforated sealed sample vials, set aside undisturbed over a period of few weeks at ambient temperature [20]. The single crystal X-ray diffraction investigation of both complexes, Me_2SnL^b and Ph_2SnL^b clearly demonstrate that they crystallized in monoclinic space groups 'P 2_1' and 'P $2_1/c$', respectively, and comprise of crystallographically discrete molecules. Table 1 organizes the relevant crystallographic data and the structure refinement parameters of both complexes. The selected bond lengths and bond angles are systematically arranged as captions of ORTEP diagram for molecular structure (Fig. 2 and Fig. 4) of complexes drawn at 30% ellipsoidal probability, along with the adopted non-hydrogen atoms labeling scheme. Fig. 2 and Fig. 4 implicitly illustrate the molecular packing, elaborately viewed

along the crystallographic axis 'b'. Undoubtedly, it is fully comprehended from the crystal structures of both complexes that ligand, N'-(5-chloro-2-hydroxybenzylidene)furan-2-carbohydrazide, H_2L^b might have preferably undergone enolisation and deprotonation prior its coordination to the organotin(IV) moiety in the presence of a proton abstractor in solution. As a result, dibasic tridentate acylhydrazone coordinates to Me_2Sn(IV) moiety or Ph_2Sn(IV) moiety via its imine nitrogen, enolic oxygen and phenolic oxygen atoms predominantly in an enol tautomeric form (as illustrated in Fig. 2 and Fig. 4). The adopted coordination mode of acylhydrazone ligand led to five- and six-membered chelate rings which deviate from planarity as shown by the measured torsions *viz.*, Sn(1)-O(2)-C(12)-C(7) 4(2), Sn(1)-N(1)-N(2)-C(1) -2.1(8), Sn(1)-N(1)-C(6)-C(7) 8(1), Sn(1)-O(1)-C(1)-N(2) -2(1) and Sn(01)-O(1)-C(1)-C(6) 17.5(3), Sn(01)-N(1)-N(2)-C(8) -8.2(2), Sn(01)-N(1)-C(7)-C(6) 1.2(3), Sn(01)-O(2)-C(8)-N(2) 7.7(3) for Me_2SnL^b and Ph_2SnL^b, respectively. The degree of distortion from an ideal geometry could conveniently be quantified in terms of the τ values ($\tau = \beta-\alpha/60$), estimated by considering two largest consecutive bond angles (β and α) around a penta-coordinated tin atom in the molecular structure [21]. The estimated 0 and 1 value for τ refer to an ideal square-pyramidal geometry and ideal trigonal-bipyramidal geometry, respectively. The respective τ values, estimated for Me_2SnL^b and Ph_2SnL^b were found to be 0.22 (τ = 154.2-141.0/60) and 0.33 (τ = 157.93-137.85/60), respectively, which strongly indicates a highly distorted square-pyramidal (SP) geometry in case of both complexes wherein the apical site was invariably occupied by the N(1) whereas the equatorial sites in the square plane were occupied by the oxygen atoms and the carbon atoms of the methyl/phenyl groups. [21]. The highly distorted square-pyramidal (SP) geometry observed in case of Me_2SnL^b and Ph_2SnL^b are on account of the peculiar bond angles which deviate from the ideal values *viz.*, C(13)-Sn(1)-C(14) 141.0(4), C(13)-Sn(1)-O(1) 95.7(5), C(13)-Sn(1)-N(1) 101.3(4), O(1)-Sn(1)-N(1) 72.32(16), O(2)-Sn(1)-O(1) 154.2(2), C(14)-Sn(1)-N(1) 117.4(5) and C(19)-Sn(01)-C(13) 137.85(8), O(1)-Sn(01)-O(2) 157.93(6), O(1)-Sn(01)-N(1) 84.26(6), C(19)-Sn(01)-N(1) 108.07(7), C(13)-Sn(01)-N(1) 113.82(7), O(2)-Sn(01)-N(1) 73.67(6), measured in the respective complexes. In the present instances, the rigidity of five- and six-membered chelate rings and the large covalent radius of the Sn(IV) atom may be thought to cause the significant deviations from ideal geometrical parameters which otherwise may constitute a perfect square-pyramidal (SP) geometry [22,23]. Additionally, there are significant covalent bonding interactions among O(1), O(2), and N(1) and Me_2Sn(IV) moiety or Ph_2Sn(IV) moiety as evident from the values of

respective bond lengths viz., Sn(1)-O(1) 2.163(4) Å, Sn(1)-O(2) 2.104(5) Å, Sn(1)-N(1) 2.203(5) Å, and Sn(01)-O(1) 2.0753(15), Sn(01)-O(2) 2.1427(14), Sn(01)-N(1) 2.1631(17) Å, measured in both complexes which exhibit a close resemblance to the sum of the covalent radii of Sn-O (2.10 Å) and Sn-N (2.15 Å) [24-26].

Insert Table 1
Insert Fig. 2

Symmetry operations:
(i) x, y, z; (ii) -x, y+1/2, -z.
Selected bond lengths (Å), bond angles (°) and torsion angles (°): Sn(1)-C(13) 2.096(11), Sn(1)-C(14) 2.100(11), Sn(1)-O(1) 2.163(4), Sn(1)-N(1) 2.203(5), Sn(1)-O(2) 2.104(5), O(1)-C(1) 1.296(7), C(12)-O(2) 1.306(8), N(1)-C(6) 1.293(9), N(2)-N(1) 1.397(7), N(2)-C(1) 1.311(8), C(7)-C(6) 1.454(10), C(1)-C(2) 1.450(8), C(13)-Sn(1)-C(14) 141.0(4), C(13)-Sn(1)-O(1) 95.7(5), C(14)-Sn(1)-O(1) 92.5(5), C(13)-Sn(1)-N(1) 101.3(4), O(1)-Sn(1)-N(1) 72.32(16), C(13)-Sn(1)-O(2) 96.3(5), C(14)-Sn(1)-O(2) 92.3(5), O(2)-Sn(1)-O(1) 154.2(2), O(2)-Sn(1)-N(1) 82.98(19), C(1)-O(1)-Sn(1) 114.5(3), C(12)-O(2)-Sn(1) 133.8(5), C(6)-N(1)-Sn(1) 127.8(4), N(2)-N(1)-Sn(1) 116.6(4), C(1)-N(2)-N(1) 110.9(5), C(12)-C(7)-C(6) 123.1(6), O(2)-C(12)-C(7) 124.0(6), N(1)-C(6)-C(7) 127.1(7), O(1)-C(1)-N(2) 125.7(5), C(14)-Sn(1)-N(1) 117.4(5), Sn(1)-O(2)-C(12)-C(7) 4(2), Sn(1)-N(1)-N(2)-C(1) -2.1(8), Sn(1)-N(1)-C(6)-C(7) 8(1), Sn(1)-O(1)-C(1)-N(2) -2(1).

Insert Fig. 3
Insert Fig. 4

Symmetry operations:
(i) x, y, z; (ii) -x, y+1/2, -z+1/2; (iii) -x, -y, -z; (iv) x, -y+1/2, z+1/2
Selected bond lengths (Å), bond angles (°) and torsion angles (°): Sn(01)-C(13) 2.124(2), Sn(01)-C(19) 2.118(2), Sn(01)-O(2) 2.1427(14), Sn(01)-N(1) 2.1631(17), Sn(01)-O(1) 2.0753(15), O(2)-C(8) 1.296(2), O(1)-C(1) 1.321(3), N(1)-C(7) 1.290(3), N(1)-N(2) 1.397(2), N(2)-C(8) 1.309(3), C(6)-C(7) 1.435(3), C(8)-C(9) 1.460(3), C(19)-Sn(01)-C(13) 137.85(8), C(13)-Sn(01)-O(2) 94.19(7), C(19)-Sn(01)-O(2) 93.03(7), C(13)-Sn(01)-N(1) 113.82(7), O(2)-Sn(01)-N(1) 73.67(6), O(1)-Sn(01)-C(13) 94.56(8), O(1)-Sn(01)-C(19) 94.00(8), O(1)-Sn(01)-O(2) 157.93(6), O(1)-Sn(01)-N(1) 84.26(6), C(8)-O(2)-Sn(01) 112.60(13), C(1)-O(1)-Sn(01) 131.26(13), C(7)-N(1)-Sn(01) 128.07(14), N(2)-N(1)-Sn(01) 115.72(13), C(8)-N(2)-N(1) 110.71(17), C(1)-C(6)-C(7) 124.28(19), O(1)-C(1)-C(6) 123.50(18), N(1)-C(7)-C(6) 126.21(19), O(2)-C(8)-N(2) 126.18(18), C(19)-Sn(01)-N(1) 108.07(7), Sn(01)-O(1)-C(1)-C(6) 17.5(3), Sn(01)-N(1)-N(2)-C(8) -8.2(2), Sn(01)-N(1)-C(7)-C(6) 1.2(3), Sn(01)-O(2)-C(8)-N(2) 7.7(3).

Insert Fig. 5

3.3. Infrared spectral studies

Some of the highly informative infrared absorptions which assist in the structural characterization of hydrazone ligands and their corresponding diorganotin(IV) derivatives are arranged in the Experimental section (spectra are illustrated in S-1 to S-14 as supporting information). The ligands seem to display IR spectral pattern which are expectedly peculiar to

similar hydrazones [27], and so a keto-imine structure is existed in the solid state (as illustrated in Fig. 1). The ν(O-H) and ν(N-H) stretching vibrations appear as well-distinguished broad and sharp bands in the frequency range 3100-3460 cm^{-1}. Well-resolved very strong and medium intensity bands located in the frequency range ca. 1672-1610 cm^{-1} may be ascribed to the $\nu(C=O)_{amido}$ and $\nu(C=N)_{azomethine}$ stretching vibrations. On the contrary, the IR spectra of the complexes do not contain ν(O-H), ν(N-H) and $\nu(C=O)_{amido}$ stretching vibrations which evidently confirm that ligands might have lost their keto-imine form as a result of enolisation and deprotonation upon complex formation with organotin moiety in the presence of a trimethylamine base as observed in the other articles [4,28]. Moreover, the $\nu(C=N)_{azomethine}$ absorption band observed in case of the ligands is markedly shifted towards the lower frequency region 1619-1580 cm^{-1} upon complexation on account of the involvement of the azomethine nitrogen in bonding to the tin atom, and also the delocalization of the electron density [29]. The characteristics weak ν(Sn-O) and ν(Sn-N) vibrational bands originated as a result of the participation of oxygen and azomethine nitrogen of the chelated ligand to the tin centers are observed in the region ~400-600 cm^{-1} [23,28]. In case of Me_2SnL^{a-c} complexes, asymmetric and symmetric ν(Sn-C) vibrational bands are seemed to display in the ranges 647-618 cm^{-1} and 583-518 cm^{-1}, respectively, which imply a non-linear Me-Sn-Me configuration. Moreover, the well-resolved stretching ν(C-H) vibrations for the butyl groups attached to organotin moiety in Bu_2SnL^{a-c} complexes can easily be observed between 2964 cm^{-1} to 2849 cm^{-1} [30]. Additionally, the ν(Sn-C) vibrations in Bu_2SnL^{a-c} complexes are observed as a weak peak at ca. 509, 518 and 521 cm^{-1}, respectively.

3.4. Multinuclear (^1H, ^{13}C, and ^{119}Sn) NMR spectral studies

3.4.1. ^1H NMR studies

^1H NMR spectral data for hydrazones and their corresponding diorganotin(IV) derivatives are arranged in the Experimental section and spectra are illustrated in S-15 to S-28 as supporting information. The resonances for hydroxyl proton, -NHN= proton and aromatic protons in the ^1H NMR spectra of the ligands are well located, and are effortlessly assigned which in turn reflect the ligands to exist in keto-imine form as shown in the Fig. 1. However, signals for the hydroxyl and -NHN= protons are expectedly disappeared in ^{1} H NMR spectra of diorganotin(IV) derivatives as a consequence of enolisation and deportation upon coordination of the ligands to the organotin(IV) moiety in the enol form as reported in the similar work [10,27]. Besides, the satellites around the

signal for azomethine proton along with significant $^{3}J(^{119}Sn\text{-}^{1}H)$ coupling constant can also be noticed on account of the coordination of the azomethine nitrogen to the tin center. Noticeable well-resolved ^{119}Sn satellites with greater $^{2}J(^{119}Sn\text{-}^{1}H)$ as compared to uncomplexed Me_2SnCl_2 ($^{2}J(^{119}Sn\text{-}^{1}H$ = 68.7) located on both sides of the singlet for Me_2Sn protons are recorded in case of the ^{1}H NMR spectra $Me_2SnL^{a\text{-}c}$. The greater $^{2}J(^{119}Sn\text{-}^{1}H)$ coupling constant as compared to that estimated in the uncomplexed Me_2SnCl_2 ($^{2}J(^{119}Sn\text{-}^{1}H$ = 68.7) is a clear indication for the higher coordination number of the tin in solution phase [31]. In dimethyltin(IV) derivatives, $CH_3\text{-}Sn\text{-}CH_3$ angles were estimated to be ca. 145.8, 145 and 155° in $(CD)_3SO$ solution upon substitution of the respective values of $^{2}J(^{119}Sn\text{-}^{1}H)$ coupling constant (= 90.5, 90.0 and 96.0 Hz) in Lockhart-Manders equation, $\theta = 0.0161\,[^{2}J(^{119}Sn\text{-}^{1}H)]^2 - 1.32\,[^{2}J(^{119}Sn\text{-}^{1}H)] + 133.4$ [32] which reflect the non-linearity of the $(CH_3)_2Sn$ moiety in the solution phase similar to the solid state. Additionally, the $CH_3\text{-}Sn\text{-}CH_3$ angle 145° estimated for Me_2SnL^{b} seems to be consistent with that observed from the X-ray diffraction analysis. The protons of butyl chains attached to tin in $Bu_2SnL^{a\text{-}c}$ complexes are recorded to exhibit their usual peculiar pattern, including a well-resolved triplet ($^{3}J_{H\text{-}H}$ = 7.3 Hz) for terminal methyl protons within δ 0.73-1.53 ppm [33]. In case of $Ph_2SnL^{a\text{-}c}$ complexes, ortho protons of phenyl groups attached to the tin center are appeared to be accompanied by ^{119}Sn satellites originated as a result of $^{1}H\text{-}^{119}Sn$ coupling. Herein, the values of $^{3}J(^{119}Sn\text{-}^{1}H)$ coupling constants were estimated to be larger than that found in uncomplexed Sn_2PhCl_2 (81.7 Hz) indicating higher coordination number of the tin in solution phase [31].

3.4.2. ^{13}C NMR studies

All characteristics ^{13}C resonances of ligands and their corresponding diorganotin(IV) derivatives are orderly arranged in a descending way in Experimental section and spectra are illustrated in S-29 to S-42 as supporting information. The signals for all carbon resonances of ligands are carefully detected, and duly assigned in their ^{13}C spectra. The peaks located at 154.02-156.44, 146.33-146.15 and 148.05-154.65 ppm for O=**C** (C-5), **C**H=N (C-6) and **C**-OH (C-12) carbons of the ligands are seemed to be reasonably shifted downfield in case of diorganotin(IV) derivatives as a consequence of the shifting of the electron-density on donor atoms to the tin center which is consistent with the earlier reports [28,34]. Furthermore, well-resolved signals for ^{13}C resonances of the alkyl/aryl groups of organotin(IV) moieties comparable to those reported for other diorganotin(IV) derivatives of the tridentate ONO dibasic ligands were successfully identified

[27,35,36].

3.4.3. ^{119}Sn NMR studies

The ^{119}Sn NMR spectral data of the diorganotin(IV) derivatives executed in a non-coordinating solvent ($CDCl_3$) are included in the Experimental section. The ^{119}Sn NMR spectra of R_2SnL^a are illustrated in Fig. 6 while those of other diorganotin(IV) derivatives are included as supporting information from S-43 to S-49. It is evident form the ^{119}Sn NMR spectra of the complexes that they adopt exclusively a monomeric structure in the solution which is in accordance with that established from single crystal X-ray diffraction analysis as there exhibit a sharp ^{119}Sn resonance peaks between δ 147.78-331.32 ppm. Besides, the sharp ^{119}Sn resonance singlets in diorganotin(IV) derivatives are observed to be shifted appreciably upfield as compared to those reported for Me_2SnCl_2 (+137 ppm), Bu_2SnCl_2 (+122 ppm), and Ph_2SnCl_2 (-32 ppm) on account of the enhancement in the co-ordination state of tin atom [31]. Additionally, these ^{119}Sn chemical shifts are observed to be peculiar to those acquired in case of other penta-coordinated diorganotin(IV) derivatives [14,16,36]. Moreover, the ^{119}Sn resonance peaks are remarkably shifted upfield in $Ph_2SnL^{a\text{-}c}$ complexes as compared those observed in alkyl organotin(IV) analogues as a consequence of the most prevalent anisotropic shielding effects and the pi-interactions observed in these cases [37].

Insert Fig. 6

3.5. Mass spectral studies

The hydrazone ligands and their corresponding diorganotin(IV) derivatives were carefully analyzed by electrospray mass spectrometry (ESMS) technique and an attempt was made to assign their true molecular weights. High resolution mass spectra (HRMS) in some of the cases were also successfully obtained, indicating the expected compounds. ESI mass spectral data are listed in the Experimental section and spectra are illustrated as supporting information form S-50 to S-71. The ESMS spectra of the studied ligands and their diorganotin(IV) derivatives are seemed to record the molecular adducts $[M+Na]^+$ and $[M+K]^+$ [38] in addition to the protonated molecular ion peaks. Besides, some of the valuable peaks were also successfully detected at m/z values ca. 192.9, 149.9, and 94.8 in the mass spectra of H_2L^a and R_2SnL^a as a consequence of the detachment of various

fragmentation species form the corresponding protonated molecular ion peaks (as shown in scheme 2). Likewise, the mass spectra of H_2L^b and R_2SnL^b were analyzed to contain the valuable ions at m/z values ca. 196.8, 153.9, and 94.7 which were conveniently identified (as shown in scheme 3). However, no any such characteristics ions with significant abundances could be detected on account of the 100 % abundant protonated molecular ion peaks in case of R_2SnL^c derivatives of H_2L^c. The first fragmentation step in each diorganotin(IV) derivative was observed to be accompanied by the prompt elimination of the R_2Sn moiety attached to the complexed ligand from its corresponding protonated molecular ion. The fragmentation mechanisms of diorganotin(IV) derivative of H_2L^a and H_2L^b invariably include a common fragmentation pattern (as shown in scheme 2 and scheme 3). The most peculiar pattern as a result of the natural abundances of Sn isotopes (^{120}Sn, ^{118}Sn, ^{116}Sn etc.) in Sn enriched species could tangibly be seen in the mass spectra of the diorganotin(IV) derivatives [39].

Insert Scheme 3

Insert Scheme 4

3.6. Thermal studies

All diorganotin(IV) derivatives were analyzed using thermogravimetric techniques (TG-DTA-DTG) in order to explore their thermal behaviour. The thermal analysis data so extracted were compiled in table S-1, and incorporated along with the pertaining thermograms (from S-72 to S-77) as supporting information. Figures 7-10 illustrate the pyrolysis curves for R_2SnL^a derivatives which seem to involve a common thermal decomposition pattern i.e. pyrolysis via two decomposition steps. In case of Me_2SnL^a, step I (20-327 °C) involves a % weight loss of 52.00 which may be ascribed to the loss of the two methyl groups attached to the Sn atom (C_2H_6) and a fraction of the ligand moiety ($C_{12}H_{10}O_2$) (calcd. % weight loss: 53.14) whereas the step II (327-464 °C) exhibits a % weight loss of 28.20 as a result of the loss of the remaining fraction of the ligand ($CN_2O_{3/2}$) and the partial sublimation of the tin metal (1/2Sn) (calcd. % weight loss: 30.3). Bu_2SnL^a seems to undergo decomposition via step I (30-321 °C, % weight loss: 44.00) and step II (321-468 °C, % weight loss: 31.70) which presumably be due to the loss of the two butyl groups attached to the Sn atom (C_8H_{18}) and a fraction of the ligand moiety (C_7H_6O) (calcd. % weight loss: 44.87), and the loss of the remaining fraction of the ligand ($C_6H_4N_2O_3$) (calcd. % weight loss: 30.96). The pyrolysis of Ph_2SnL^a includes loss of the two phenyl groups attached to the Sn atom (C_6H_{10}) and a

fraction of the ligand moiety (CH_3O) (calcd. % weight loss: 34.86) in the step I (28-343 °C, % weight loss: 34.9) followed by the subsequent loss of the remaining ligand moiety ($C_{12}H_8N_2O_3$) (calcd. % weight loss: 35.99) in step II (327-482 °C, % weight loss: 35.99). The decomposition of Oct_2SnL^a consists of loss of the two octyl chains attached to the Sn atom (calcd. % weight loss: 37.46) in the first step (calcd. % weight loss: 36.5) followed by the elimination of the whole ligand moiety ($C_{13}H_{11}N_2O_3$) (calcd. % weight loss: 40.07) in step II (327-482 °C, % weight loss: 38.3). The thermal behaviour of Me_2SnL^b and Ph_2SnL^b derivatives seems not to be consistent as perceived from the figures S-72 and S-73. The first step (20-458 °C, % weight loss: 83.7) for Me_2SnL^b includes the loss of two methyl groups attached to the Sn atom (C_2H_6) along with the whole ligand moiety ($C_{12}H_7ClN_2O_{3/2}$) followed by sublimation of the tin atom (calcd. % weight loss: 83.63). Herein, second step (458-642 °C, % weight loss: 6.3) may be considered on account of the sublimation of the tin element (25-356 °C, % weight loss: 6.55). However, the pyrolysis curve of Ph_2SnL^b involves a loss of a fraction of the ligand moiety ($C_{11}H_8ClO$) (calcd. % weight loss: 35.77) in step I (25-356 °C, % weight loss: 36.1), and a subsequent loss of two phenyl groups attached to the Sn atom ($C1_2H_{10}$) along with the remaining fraction of the ligand (calcd. % weight loss: 39.24) in the step II (356-570°C, % weight loss: 39.6). The first step (27-387 °C, % weight loss: 62.6) in the pyrolysis of Me_2SnL^c may be ascribed to the elimination of both methyl groups attached to the Sn atom (C_2H_6) along with the whole ligand moiety ($C_{12}H_7N_3O_3$) (calcd. % weight loss: 64.24) whereas the second step (387-458 °C, % weight loss: 12.8) is attributed to the partial sublimation of the tin element (calcd. % weight loss: 11.90). The pyrolysis curves of Bu_2SnL^c and Ph_2SnL^c, however consists of three decomposition steps. In the first step (36-293 °C, % weight loss: 15.6) of Bu_2SnL^c, a fraction of the ligand (C_5H_3O) may be considered to evolve out (calcd. % weight loss: 15.63). The second step (293-447 °C, % weight loss: 40.5) involve the elimination of one of the butyl group (C_4H_9) attached to the Sn atom along with the remaining fraction of the ligand ($C_7H_4N_2O_2$) (calcd. % weight loss: 40.54). Finally, in the third step (447-507 °C, % weight loss: 15.9), the second butyl group (C_4H_9) and one molecule of oxygen are evolved out (calcd. % weight loss: 17.60). The pyrolysis curves of Ph_2SnL^c may be divided in to three decomposition steps viz., step I (26-327 °C, % weight loss: 15.6), step II (327-438 °C, % weight loss: 32.0) and step III (438-486 °C, % weight loss: 23.5) which are probably ascribed to the loss of a fraction of the ligand moiety (C_5H_3O) (calcd. % weight loss: 14.48), the loss of the remaining fraction of the ligand moiety ($C_7H_4N_3O_3$) (calcd. % weight loss: 32.61) and the two phenyl groups attached to the

Sn atom ($C_{12}H_{10}$) (calcd. % weight loss: 28.23) respectively. The pyrolysis of Oct_2SnL^c consists of two steps; 28-300 °C and 300-500 °C which may be attributed to the loss of a fraction of the ligand moiety (obsd. % weight loss: 15.43, calcd. % weight loss: 15.38) and the loss of the two octyl chains attached to the Sn atom along with the remaining fraction of the ligand moiety ($C_7H_4N_2O_2$) (obsd. % weight loss: 60.42, calcd. % weight loss: 60.57) respectively. In the later stages of pyrolysis of diorganotin(IV) derivatives, the characteristic broad exothermic peaks were also noticed in their DTA curves which infer the oxidation of tin metal content to tin dioxide as residue, comparable to our previous works [40-42].

Insert Fig. 7

Insert Fig. 8

Insert Fig. 9

Insert Fig. 10

4. Conclusion

In a nut shell, facile synthesis and chracterization of three acylhydrazones viz., N'-(2-hydroxy-3-methoxybenzylidene)furan-2-carbohydrazide, N'-(5-chloro-2-hydroxy-benzylidene)furan-2-carbo-hydrazide and N'-(2-hydroxy-5-nitrobenzylidene)furan-2-carbohydrazide and their eleven new diorganotin(IV) derivatives have been described. Two mononuclear complexes, Me_2SnL^b and Ph_2SnL^b have been investigated by single crystal X-ray diffraction to adopt a highly distorted square-pyramidal geometry (SP) wherein the imine nitrogen preferably occupies the apical site whereas the more electronegative enolic and phenolic oxygen atoms of the tridentate chelating ligand and two carbon atoms of the methyl/phenyl groups of the organotin(IV) moiety, $[R_2Sn(IV)]^{2+}$ align themselves equatorially around the five-coordinated tin center in a square plane. Thermal stability and decomposition trends of diorganotin(IV) derivatives indicate almost same pattern in the most of the cases which involves the loss of organic groups attached to tin followed by the decomposition of the ligand moiety.

Acknowledgements

The authors are thankful to the Head, Institute Instrumentation Centre (IIC), Indian Institute of Technology Roorkee, Roorkee, India for providing facilities to carry out single crystal X-ray study and thermal studies. One of the authors (Mr. Sundeep Kumar) is thankful to All India Council for

Technical Education (AICTE), New Delhi, India, for financial support under quality improvement programme (QIP).

Appendix A. Supplementary material

CCDC 1477450 and CCDC 1496981 contain the supplementary crystallographic data for this paper. These data can be obtained free of charge from The Cambridge Crystallographic Data Centre via www.ccdc.cam.ac.uk/data_request/cif. A supplementary file contains IR, ^{1}H, ^{13}C and ^{119}Sn NMR, and ESMS spectra, TG-DTA-DTG thermograms of all compounds.

Refrences

[1] D.S. Kalinowski, P.C. Sharpe, P.V. Bernhardt, D.R. Richardson, J. Med. Chem. 51(2007) 331.

[2] C. Congiu, V. Onnis, Bioorg. Med. Chem. 21 (2013) 6592.

[3] P. Melnyk, V. Leroux, C. Sergheraert, P. Grellier, Bioorg. Med. Chem. Lett. 16 (2006) 31.

[4] T. Sedaghat, M. Yousefi, G. Bruno, H.A. Rudbari, H. Motamedi, V. Nobakht, Polyhedron 79 (2014) 88.

[5] M. Hong, H. Yin, X. Zhang, C. Li, C. Yue, S. Cheng, J. Organomet. Chem. 724 (2013) 23.

[6] M. Hong, H. Geng, M. Niu, F. Wang, D. Li, J. Liu, H. Yin, Eur. J. Med. Chem. 86 (2014) 550.

[7] C. Pellerito, L. Nagy, L. Pellerito, A. Szorcsik, J. Organomet. Chem. 691 (2006) 1733.

[8] X. Song, A. Zapata, G. Eng, J. Organomet. Chem. 691 (2006) 1756.

[9] H. D. Yin, S. W. Chen, L. W. Li, D. Q. Wang, Inorg. Chim. Acta 360 (2007) 2215.

[10] T. Sedaghat, L. Tahmasbi, H. Motamedi, R. Reyes-Martinez, D. Morales-Morales, J. Coord. Chem. 66 (2013) 712.

[11] H.D. Yin, M. Hong, Q.B. Wang, S.C. Xue, D.Q. Wang, J. Organomet. Chem. 690 (2005) 1669.

[12] H. Yin, J. Li, M. Hong, J. Cui, L. Dong, Q. Zhang, J. Mol. Struct. 985 (2011) 261.

[13] M. Hong, H.-D. Yin, J.-C. Cui, Solid State Sci. 13 (2011) 501.

[14] D. K. Dey, S. P. Dey, A. Lycka, G. M. Rosair, Polyhedron 30 (2011) 2544.

[15] B. Samanta, J. Chakraborty, D. K. Dey, V. Gramlich, S. Mitra, Struct. Chem. 18 (2007) 287.

[16] T. Sedaghat, Y. Ebrahimi, L. Carlucci, D. M. Proserpio, V. Nobakht, H. Motamedi, M. R. Dayer, J. Organomet. Chem. 794 (2015) 223.

[17] H.E. Gottlieb, V. Kotlyar, A. Nudelman, J. Org. Chem. 62 (1997) 7512.

[18] A. Altomare, G. Cascarano, C. Giacovazzo, A. Guagliardi, M.C. Burla, G. Polidori, M. Camalli, SIRPOW.92 - a program for automatic solution of crystal structures by direct methods optimized for powder data, J. Appl. Crystallogr. 27 (1994) 435.

[19] G. Sheldrick, SHELX-97, program for the solution and refinement of crystal structures, University of Göttingen, Germany (1997).

[20] W. Clegg, in: J. A. McCleverty, T. J. Meyer (Eds), Cophrehensive Coord. Chem. II, 1 (2003) 579.

[21] A.W. Addison, T.N. Rao, J. Reedijk, J. Van Rijn, G.C. Verschoor, J. Chem. Soc, Dalton Trans. 7 (1984) 1349.
[22] S. Öztaş, E. Şahin, N. Ancın, S. Ide, M. Tüzün, J. Mol. Struct. 705 (2004) 107.

[23] C. Pettinari, F. Marchetti, R. Pettinari, D. Martini, A. Drozdov, S. Troyanov, Inorg. Chim. Acta 325 (2001) 103.

[24] R. Zhang, Q. Wang, Q. Li, C. Ma, Inorg. Chim. Acta 362 (2009) 2762.

[25] M. Affan, M. Salam, F.B. Ahmad, J. Ismail, M.B. Shamsuddin, H.M. Ali, Inorg. Chim. Acta 366 (2011) 227.

[26] M.A. Affan, S.W. Foo, I. Jusoh, S. Hanapi, E.R. Tiekink, Inorg. Chim. Acta 362 (2009) 5031.

[27] T. Sedaghat, A. Tarassoli, Z. Ansari-Asl, H. Motamedi, J. Coord. Chem. 66 (2013) 2549.

[28] H.D. Yin, M. Hong, G. Li, D.Q. Wang, J. Organomet. Chem. 690 (2005) 3714.

[29] H.Yin, J. Cui, Y. Qiao, Polyhedron 27 (2008) 2157.

[30] D.K. Dey, S.P. Dey, N.K. Karan, A. Lyčka, G.M. Rosair, J. Organomet. Chem. 749 (2014) 320.

[31] A.G Davies, Organotin Chemsitry, second ed., Wiley-VCH, Weinheim, 2004.

[32] T.P. Lockhart, W.F. Manders, Inorg. Chem. 25 (1986) 892.

[33] M. Nath, R. Yadav, M. Gielen, H. Dalil, D. de Vos, G. Eng, Synthesis, Appl. Organomet. Chem. 11(1997) 727.

[34] B. Wrackmeyer, Ann. Rept. NMR Spectrosc. 16 (1985) 73.

[35] S. Shujah, Z. Rehaman, N. Muhammad, S. Ali, N. Khalid, M. N. Tahir, J. Organomet. Chem. 696 (2011) 2772.

[36] S. Shujah, A. Shah, Z. Rehaman, N. Muhammad, S. Ali, R. Qureshi, N. Khalid, A. Meetsma, Eur. J. Med. Chem. 45 (2010) 2902.

[37] S. Shujah, Z. Rehman, N. Muhammad, A. Shah, S. Ali, N. Khalid, A. Meetsma, J. Organomet. Chem. 741 (2013) 59.

[38] W. Henderson, B.K. Nickleson, L.J. McCaffrey, Polyhedron 17 (1998) 4291.

[39] R. Jirásko, M. Holčapek, Mass Spectrom. Rev. 30 (2011) 1013.

[40] M. Nath, P.K. Saini, A. Kumar, Appl. Organomet. Chem. 23(2009) 434.

[41] M. Nath, P.K. Saini, A. Kumar, J. Organomet. Chem. 695 (2010) 1353.

[42] S. Kumar, M. Nath, J. Organomet. Chem. 848 (2017) 10.

Legends of Figures and Schemes

Fig. 1. Structures of acylhydrazone Schiff base ligands along with the atomic labeling scheme for nmr assignments.

Fig. 2. ORTEP diagram of Me_2SnL^b along with the adopted non-hydrogen atoms labeling scheme. The ellipsoids are displayed at 30% probability level and hydrogen atoms are not included for clarity.

Fig. 3. The molecular packing of viewed Me_2SnL^b along the crystallographic axis 'b'.

Fig. 4. ORTEP diagram of Ph_2SnL^b along with the adopted non-hydrogen atoms labeling scheme. The ellipsoids are displayed at 30% probability level and hydrogen atoms are not included for clarity.

Fig. 5. The molecular packing of viewed Ph_2SnL^b along the crystallographic axis 'b'.

Fig. 6. ^{119}Sn NMR spectra of R_2SnL^a complexes.

Fig. 7. TG-DTA-DTG thermograms of Me_2SnL^a.

Fig. 8. TG-DTA-DTG thermograms of Bu_2SnL^a.

Fig. 9. TG-DTA-DTG thermograms of Ph_2SnL^a.

Fig. 10. TG-DTA-DTG thermograms of Oct_2SnL^a.

Scheme 1. Systematic numbering scheme of the organic groups attached to Sn atom in diorganotin(IV) derivatives.

Scheme 2. Systematic synthetic route for acylhydrazone and their corresponding diorganotin(IV) derivatives.

Scheme 3. A plausible fragmentation mechanism for dimethyltin(IV) complex of *(2-hydroxy-3-methoxybenzylidene)furan-2-carbohydrazide* ligand.

Scheme 4. A plausible fragmentation mechanism for dimethyltin(IV) complex of *N'-(5-chloro-2-hydroxybenzylidene)furan-2-carbohydrazide*.

Table 1
Crystallographic data and structure refinement parameters for Me_2SnL^b and Ph_2SnL^b.

	Me_2SnL^b	**Ph_2SnL^b**
Empirical formula	$C_{12}H_{13}ClN_2O_3Sn$	$C_{24}H_{17}ClN_2O_3Sn$
Formula weight	411.42	535.56
Crystal system	monoclinic	monoclinic
Space group	'P 21'	'P 21/c'
	a (Å) = 6.433 (5)	a (Å) = 8.8238 (4)
	b (Å) = 7.509 (5)	b (Å) = 18.6665 (8)
	c (Å) = 15.817 (5)	c (Å) = 13.3236 (6)
	β (°) = 95.873 (5)	β (°) =101.0040 (10)
V(Å^3)	760.0 (8)	2154.17 (17)
Z	2	4
d (g cm^{-3})	1.798	1.651
μ (Mo k$_\alpha$) (mm^{-1})	1.867	1.339
F(000)	404	1064
T(K)	293 (2)	293 (2)
Wavelength, λ (Å)	0.71073	0.71073
θ Minimum-maximum(°)	3.37-26.67	1.901-28.303
Independent reflections/ total reflections	3374	5356
Reflections collected	11339	28724
Limiting indices	$-7 \le h \le 8$,	$-11 \le h \le 11$,
	$-10 \le k \le 9$,	$-24 \le k \le 21$,
	$-20 \le l \le 21$	$-17 \le l \le 17$
Data/restraints/parameters	3708/1/194	5356/0/284
Final R indices [I>2σ(I)]	R_1 = 0.0324	R_1 = 0.0248
	wR_2 = 0.0864	wR_2 = 0.0571
R indices (all data)	R_1 = 0.0373	R_1 = 0.0333
	wR_2 = 0.0920	wR_2 = 0.0618
Largest diff. peak and hole (e.A^{-3})	1.104, -1.055	0.450, -0.474
Goodness-of-fit (GOF) on F2	1.119	1.089
Flack Parameter	0.143(14)	-

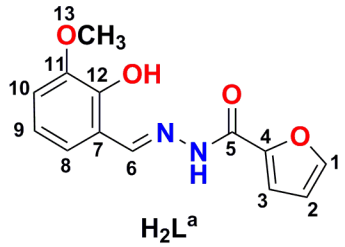

H_2L^a

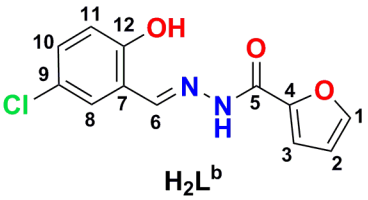

H_2L^b

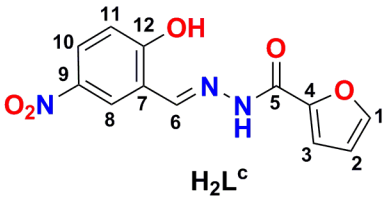

H_2L^c

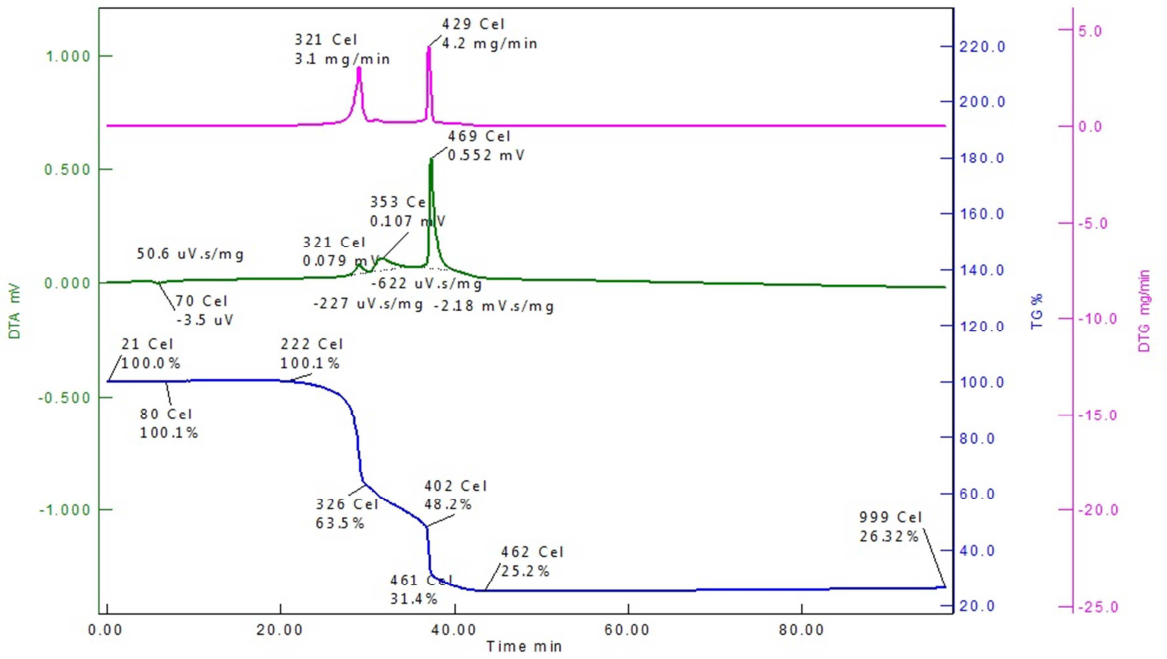

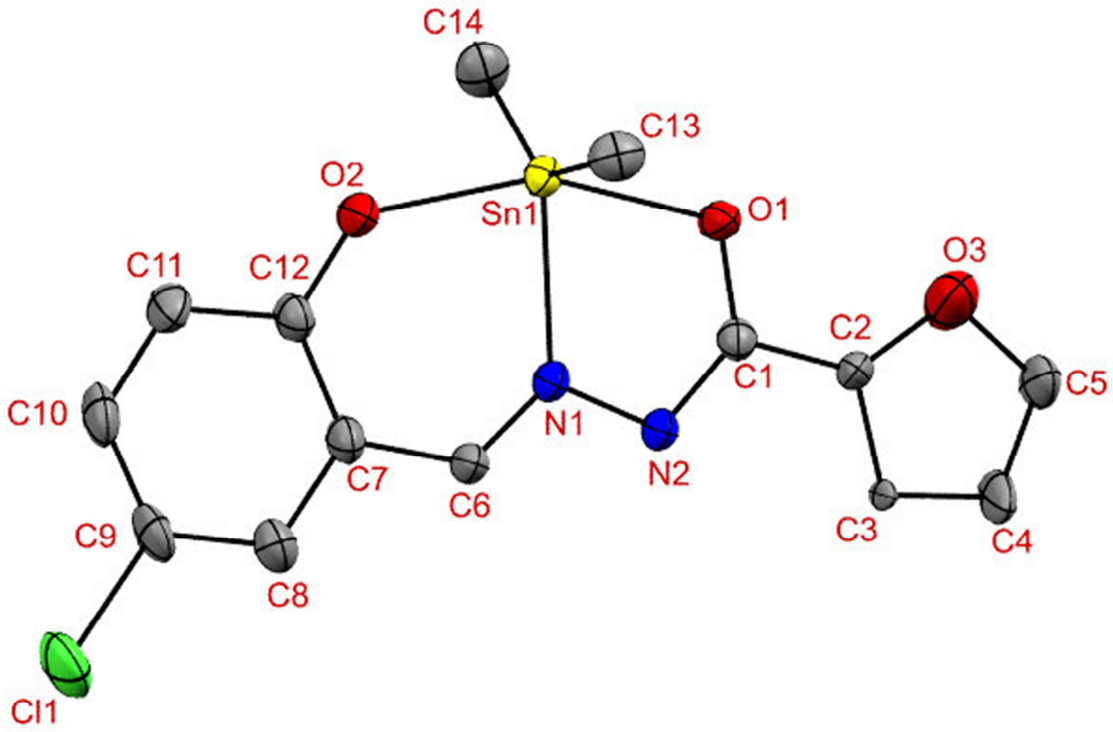

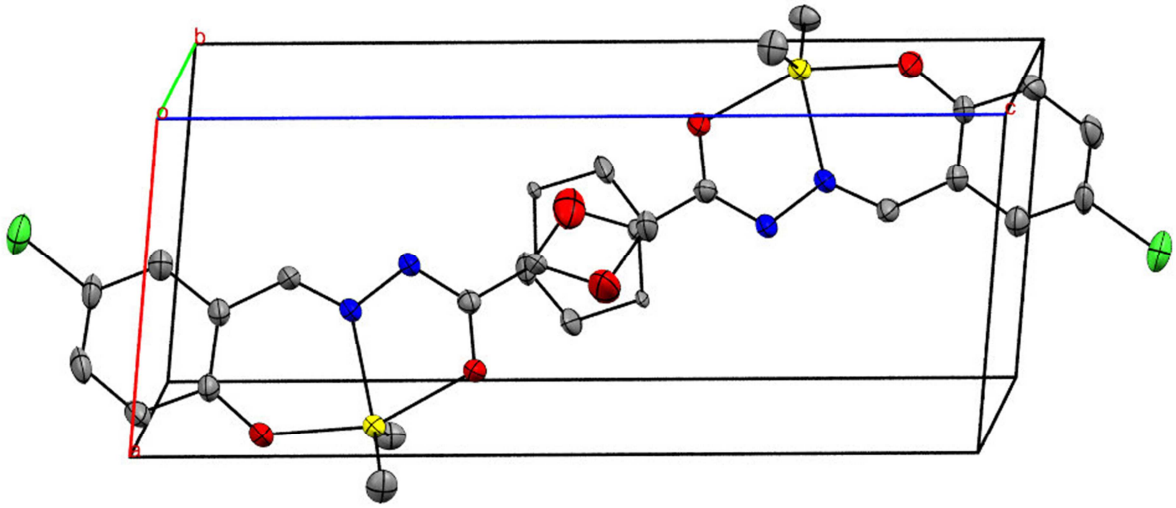

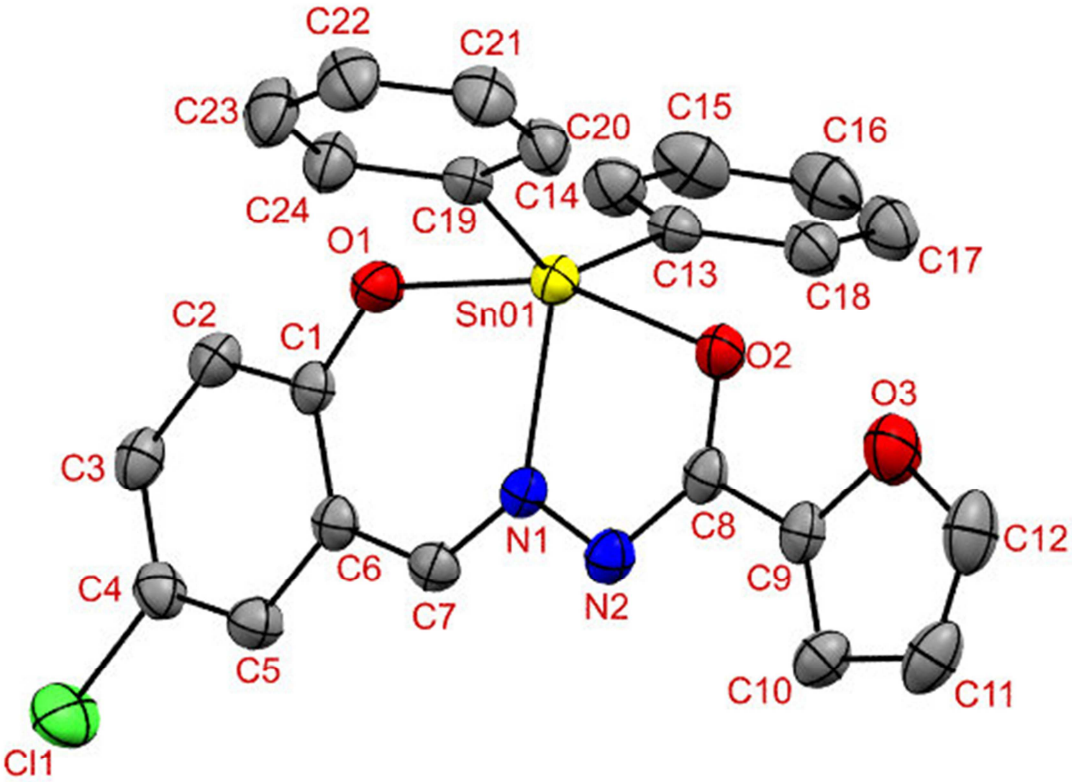

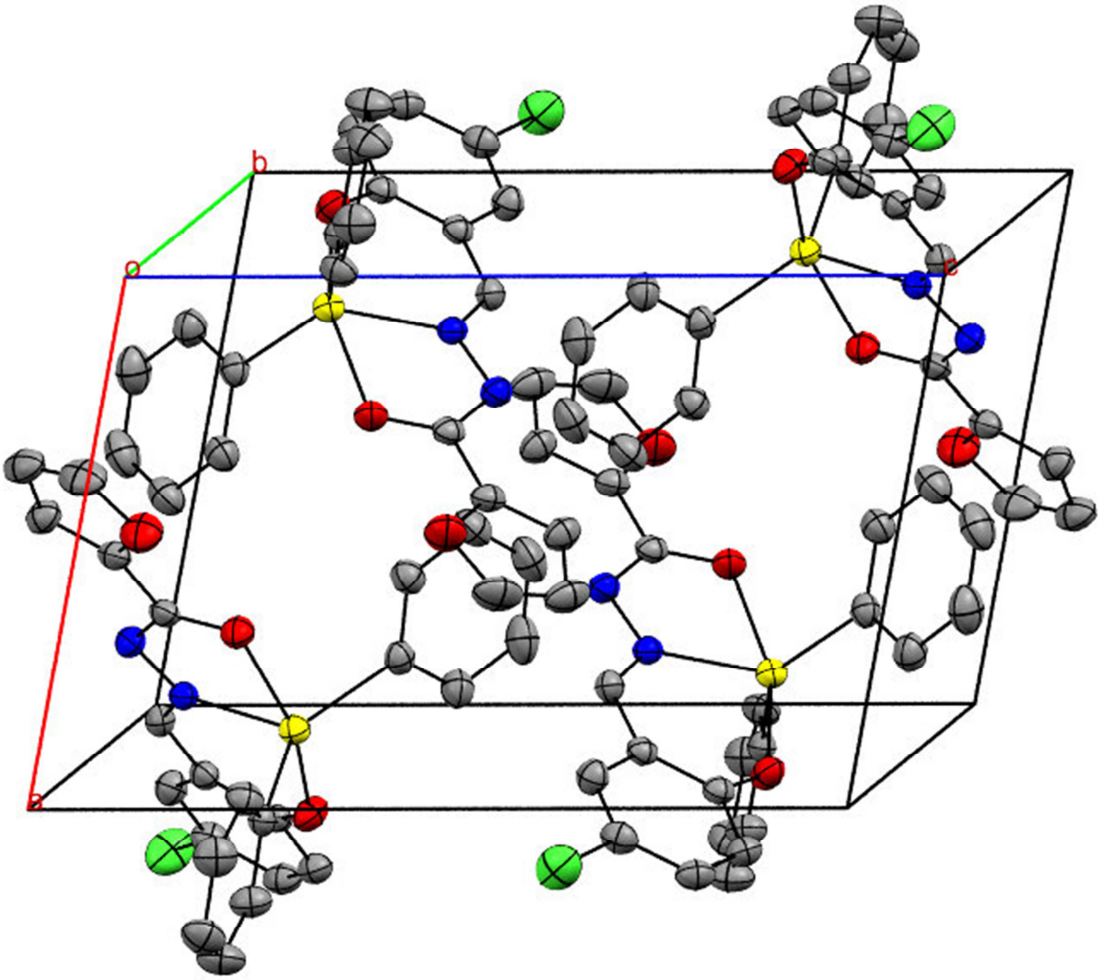

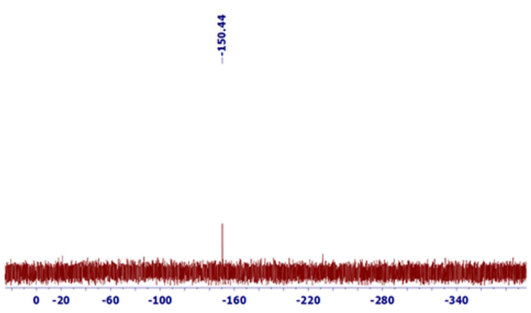

a) Me_2SnL^a

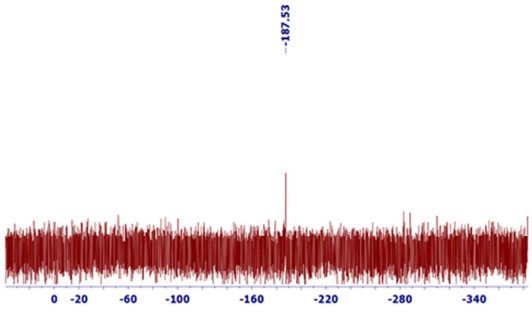

b) Bu_2SnL^a

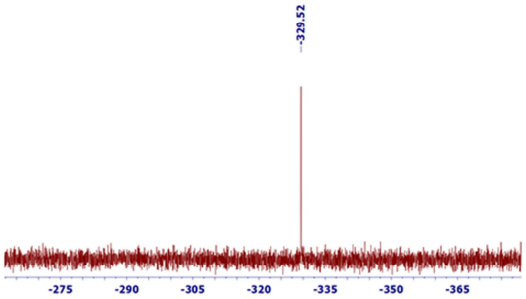

c) Ph_2SnL^a

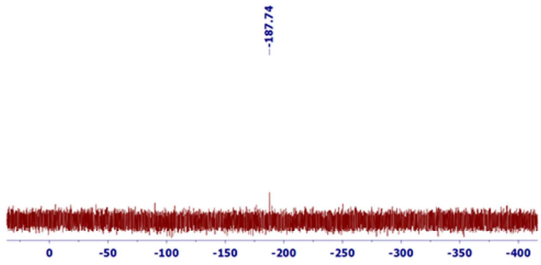

d) Oct_2SnL^a

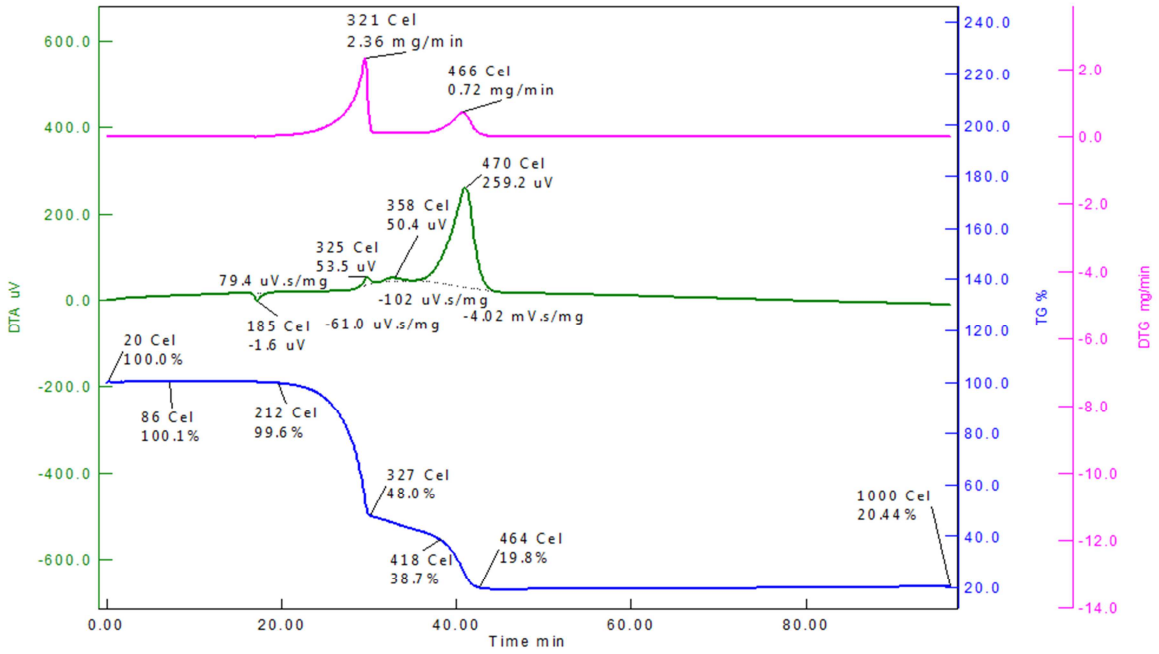

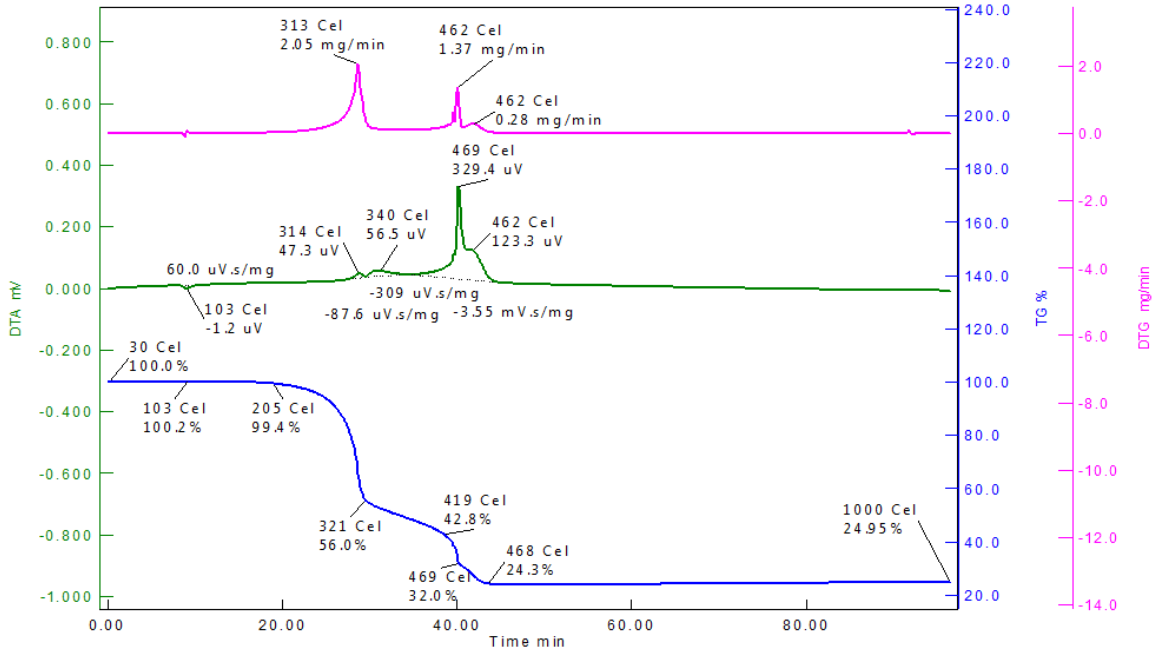

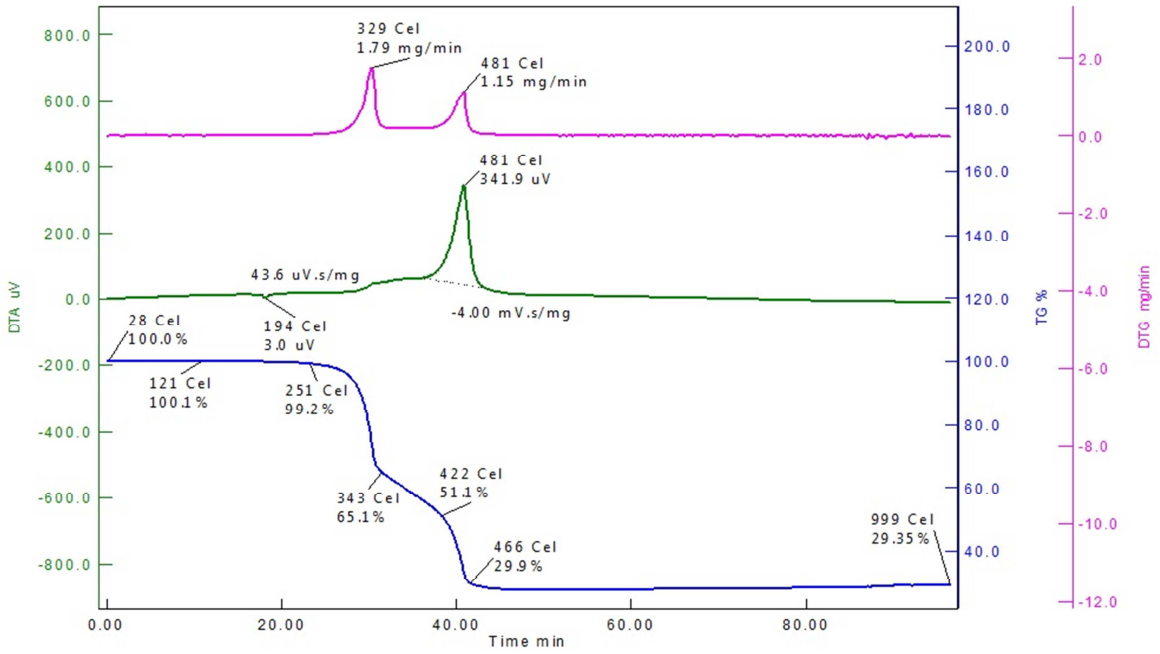

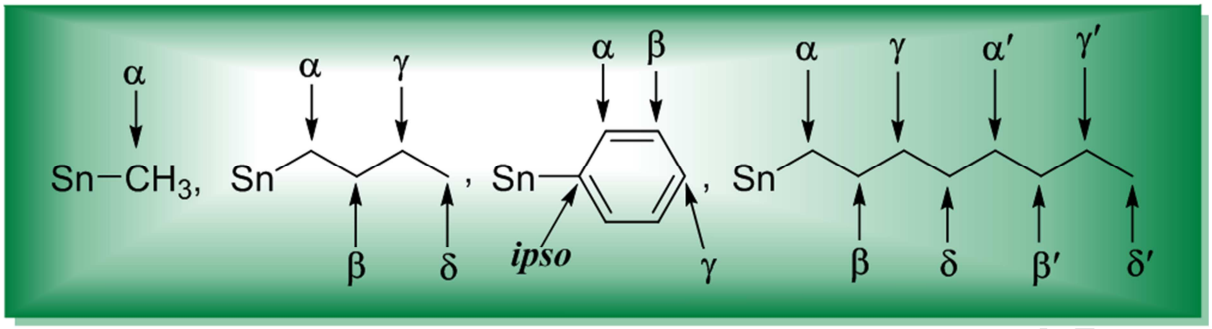

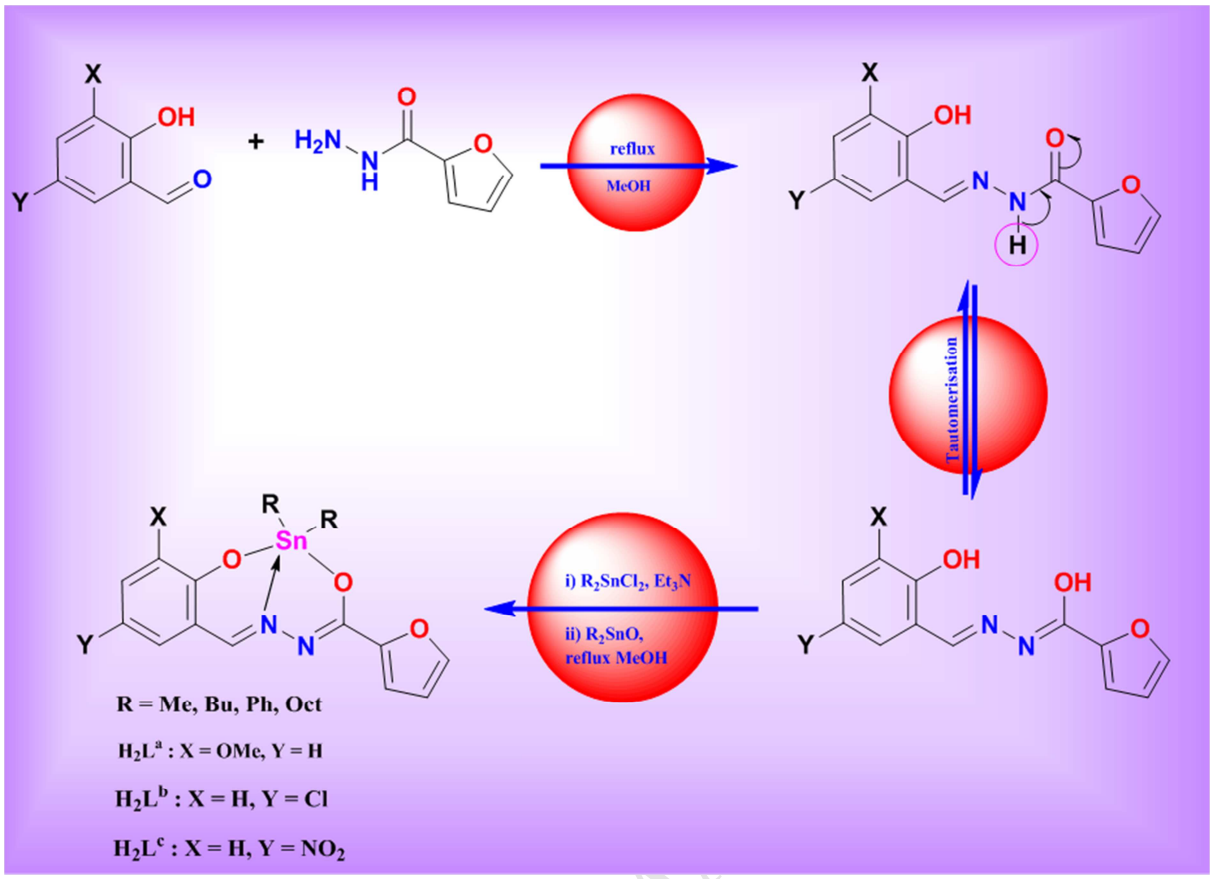

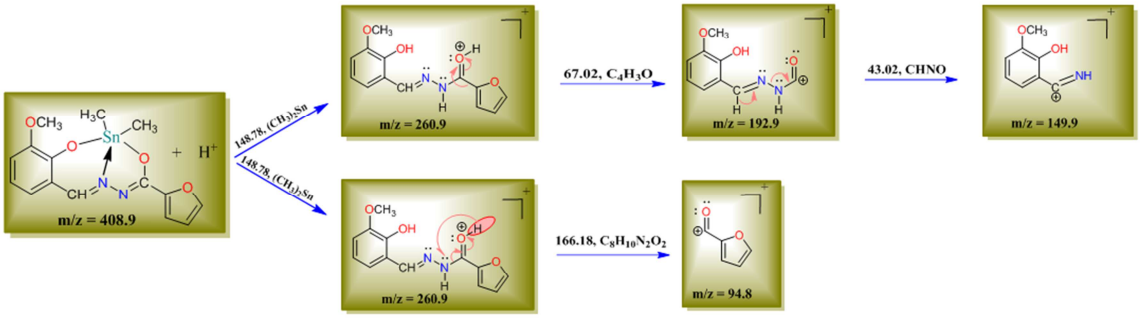

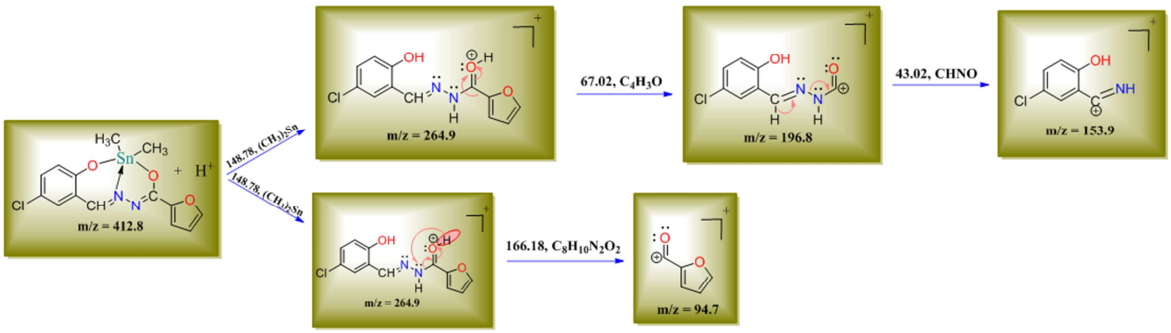

Research Highlights

- Some new organotin(IV) complexes of acylhydrazones have been synthesized in the presence of triethylamine base.
- Their geometry has been investigated by various spectroscopic techniques.
- Single crystal X- ray diffraction analysis demonstrates a highly distorted square-pyramidal geometry (SP) around tin.
- Their thermal stability and decomposition trends have also been elucidated in air by thermo-gravimetric (TG, DTG and DTA) techniques